A coupled model of transport-reaction-mechanics with trapping, Part II: Large strain analysis

Matteo Arricca [a], Luigi Cabras [b], Mattia Serpelloni [a,b], Claudia Bonanno [a,c], Robert M. McMeeking [a,d,e,f], Alberto Salvadori [a,b,*]

[a] *The Mechanobiology research center, UNIBS - Brescia, 25123, Italy*
[b] *Department of Mechanical and Industrial Engineering, Università degli Studi di Brescia, via Branze 38, 25123 Brescia, Italy*
[c] *Department of Civil, Environmental, Architectural Engineering and Mathematics, Università degli Studi di Brescia, via Branze 43, 25123 Brescia, Italy*
[d] *Materials and Mechanical Engineering Departments, University of California, Santa Barbara, CA 93106, USA*
[e] *School of Engineering, University of Aberdeen, King's College, Aberdeen AB24 3UE, UK*
[f] *INM - Leibniz Institute for New Materials, Campus D2 2, Saarbruecken, Germany*

ARTICLE INFO

Keywords:
Chemo-transport-mechanics
Thermodynamics of continua
Finite strains
Finite elements

ABSTRACT

A coupled finite strain chemo-transport-mechanical formulation with trapping is here proposed to extend a previous work set in the realm of small strain theory in continuum mechanics. The theory is rooted in non-equilibrium rational thermodynamics. The kinematics is based on a multiplicative decomposition of the deformation gradient to account for swelling and shrinking, thermal, elastic and inelastic contributions. Mass balance laws and balance of linear and angular momentum, as well as the laws of thermodynamics for a convecting body, are directly formulated in their material description, after specifications of some standard transformation rules between current and reference configuration. Thermodynamic restrictions are identified based on the functional dependence of the referential Helmholtz free energy density, which is chosen as the thermodynamic potential, and further subjected to a constitutive additive decomposition. Constitutive prescriptions for the chemical potentials, referential heat and mass fluxes, chemical kinetics and the generalized heat equation lead to the establishment of the governing equations. The theoretical framework is complemented by numerical simulations, highlighting the potential of the proposed formulation in multi-physics applications.

1. Introduction

Multi-physics frameworks, by their own nature, account for several phenomena and model several processes at different scales, with the common need to couple effects arising from the different physical activities that contribute to each process. The proposed finite strain coupled model of transport-reaction-mechanics with trapping originates as a natural extension of a previous work (Salvadori et al., 2018b) developed in the realm of small strain theory in continuum mechanics. Chemo-thermo-mechanics is usually coupled with mass transport, driven by a single effect like diffusion or migration (or a combination of both) and, less often, with trapping and/or a mass source term to account for mass conversion. The trapping process diminishes the availability of transported species that, once trapped, are usually assumed to stay immobilized. Heat fluxes and sources, mechanical surface and body forces, as standard in thermo-mechanics, complete the framework.

---

[*] Corresponding author at: The Mechanobiology research center, UNIBS - Brescia, 25123, Italy.
E-mail address: alberto.salvadori@unibs.it (A. Salvadori).

The coupling of chemo-thermo-mechanics with trapping allows the description of several multi-disciplinary applications. For instance, in the realm of mechanobiology, the conversion of free to trapped proteins (Bell, 1978; Boulbitch et al., 2001; Freund and Lin, 2004; Shenoy and Freund, 2005; Liu et al., 2007; Golestaneh and Nadler, 2016; Arricca et al., 2022; Serpelloni et al., 2022) allows cell adhesion, mediated by chemical interactions between freely mobile receptors along a cell membrane and ligands located either on a substrate or onto another adjacent cell surface. Typically, the interaction of mobile high affinity integrins and specific proteins embedded in the extra-cellular matrix immobilize integrins in multi-molecular plaques termed focal adhesions (Deshpande et al., 2007, 2008; McMeeking and Deshpande, 2017; Vernerey and Farsad, 2014; Cheng et al., 2009; Serpelloni, 2020). Similarly, the interplay between the Vascular Endothelial Growth Factor Receptor 2 (VEGFR2) along endothelial cell membranes and growth factor molecules released by cancer cells traps VEGFR2 (Serpelloni et al., 2020; Damioli et al., 2017; Salvadori et al., 2018a). In actin diffusion and polymerization to form cytoskeletal structures in the cell cytosol, the trapping process is associated with a change of phase of the actin protein, from globular to filamentous form (Serpelloni et al., 2021).

Other multi-disciplinary applications of chemo-thermo-mechanics with trapping can be found in the exposure of metals to hydrogen gas. In storage tanks, hydrogen atoms diffuse within the crystalline structure of the metal and are trapped in defects (McNabb and Foster, 1963; Oriani, 1970; Hirth, 1980; Sofronis and McMeeking, 1989; Kumnick and Johnson, 1980; Krom et al., 1999; Krom and Bakker, 2000; Toribio and Kharin, 2015). The charge–discharge of batteries is due to the motion of ions, leads to the being immobilized in active particles after their insertion into the electrodes (Zhang and White, 2007; Liu et al., 2012; Pharr et al., 2012; Zhao et al., 2012; McDowell et al., 2013; Wang et al., 2013; Drozdov, 2014; Ganser et al., 2019; Cabras et al., 2022a,b; Magri et al., 2022). Chemo-active soft materials with coexistent diffusion and reaction of species can induce a crosslinking mechanism or the inclusion of molecules in the polymer network (as in polymer gel membranes and/or hydrogels) (Lucantonio et al., 2016; Bacca and McMeeking, 2017; Bacca et al., 2019; Zhong et al., 2021; Hajikhani et al., 2021; Narayan and Anand, 2022). Further examples of chemo-thermo-mechanics with trapping are represented by vacancies and dendritic growth, solid propellant, bio-electrochemistry, solute solidification, moisture diffusion in polymer nanocomposites.

Following the same path of reasoning of Salvadori et al. (2018b), we use the network model proposed by Larche and Cahn (1973); it is therefore assumed that the freely diffusive species move in the network (lattice sites) of the hosting material, until immobilized via chemical reactions in specific trap sites, isolated from one another. This implies that the body being analyzed is the host material and that the spatial mappings, deformation gradients, etc., are defined for the host material. The trapping process is commonly associated with a separation of phases, or a change of phase, and determined by species chemical interactions. The diffusion process of species is affected by the trapping process (and vice-versa) by means of a change in the concentration gradient.

The kinetic process of trapping, involving chemical reactions, is well described by appropriately modifying the *van't Hoff* mass action law to account for elastic and swelling contributions, and set in a well-established thermodynamic framework (De Groot and Mazur, 1984; DeHoff, 2006). A swelling phenomenon, due to the trapping process, may generate large mechanical stress and strain in the material, affecting all other processes due to a coupling with the chemo-thermo-mechanics; these interactions are accounted for, within a rigorous thermodynamic setting (Gurtin et al., 2010; Tadmor et al., 2011), in the field of finite strain theory in continuum mechanics.

The manuscript is organized as follows. Section 2 provides some standard definitions to facilitate the exposition of the formulation in the field of finite strain mechanics. Assumptions on kinematics, in terms of multiplicative decomposition of the deformation gradient, and the resulting volumetric Jacobian and velocity gradient, are presented in Section 3. Mass balance equations and the laws of continuum mechanics are introduced in Section 4. Section 5 is dedicated to the laws of thermodynamics, and to exploiting thermodynamic prescriptions by means of the Coleman–Noll procedure, under the assumption of Curie's symmetry principles. Constitutive theory is discussed in Section 6, based on an additive decomposition of the referential Helmholtz free energy density, providing consistent phenomenological specifications for all contributions to the free energy, stress tensor, chemical potentials, heat and mass fluxes. Chemical kinetics and governing equations in Sections 7 and 8 anticipate numerical simulations of a focused ion beam mass implantation into a spherical particle, with results described in Section 9. Concluding remarks complete the paper.

2. Definitions

2.1. Motion and deformation gradient

Let $\mathcal{B}_t \in \mathbb{R}^3$ denote the spatial description of an advecting volume, whose boundary is $\partial\mathcal{B}_t$. Let $\mathcal{B}$ and $\partial\mathcal{B}$ indicate their referential counterparts, as standard in finite strain mechanics (Gurtin et al., 2010; Tadmor et al., 2011). The transformation of a material point $\vec{X} \in \mathcal{B}$ into a spatial point $\vec{x} \in \mathcal{B}_t$, is described by means of a smooth function $\vec{\chi}(\vec{X}, t)$

$$\vec{x} = \vec{\chi}(\vec{X}, t) \; ,$$

which is a one-to-one map representing the motion of $\vec{X} \in \mathcal{B}$ at time t. We will also assume that $\mathcal{B}_t$ at $t = 0$ coincides with $\mathcal{B}$, *i.e.*, for all material points $\vec{X} = \vec{\chi}(\vec{X}, 0)$. The material velocity is given by $\dot{\vec{\chi}}(\vec{X}, t)$, whereas displacements write as $\vec{u} = \vec{\chi} - \vec{X}$.

At a fixed time t, we will name

$$\mathbf{F} = \mathrm{Grad}\left[\, \vec{\chi}(\vec{X}, t) \,\right] \; , \tag{1}$$

the deformation gradient, *i.e.*, $\mathrm{F}_{ij} = \partial\chi_i / \partial X_j$. Only motions such that

$$J = \det[\,\mathbf{F}\,] > 0$$

are admissible, in order to avoid total material compaction (see Gurtin et al. (2010)).

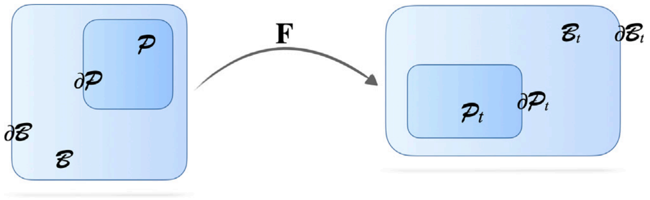

Fig. 1. Schematic representation of the material and spatial configuration $\mathcal{B}$ and $\mathcal{B}_t$, with boundaries $\partial\mathcal{B}$ and $\partial\mathcal{B}_t$, and of a generic sub-part $\mathcal{P}_t \subset \mathcal{B}_t$, image of $\mathcal{P} \subset \mathcal{B}$, with boundaries $\partial\mathcal{P}_t$ and $\partial\mathcal{P}$, respectively.

2.2. Transformation rules

Denote with $\mathcal{P}_t \subset \mathcal{B}_t$ an arbitrary region image of $\mathcal{P} \subset \mathcal{B}$, and with $\partial\mathcal{P}_t$ and $\partial\mathcal{P}$ their respective boundaries (see Fig. 1). Let $\phi(\vec{x},t) \in \mathcal{P}_t$ and $\phi_R(\vec{X},t) \in \mathcal{P}$ be two generic tensorial functions of any order. If

$$\int_{\mathcal{P}_t} \phi(\vec{x},t)\,\mathrm{d}v = \int_{\mathcal{P}} \phi_R(\vec{X},t)\,\mathrm{d}V\ , \tag{2}$$

then the following transformation rule applies

$$\phi_R(\vec{X},t) = J(\vec{X},t)\,\phi(\vec{x}(\vec{X},t),t)\,. \tag{3}$$

Let $\vec{\varphi}(\vec{x},t)$ be a spatial vector, and $\vec{x}$ a point on an oriented surface $\partial\mathcal{P}_t$ defined by the direction of the outward normal vector $\vec{n}$. Denote with $\vec{n}_R$ the outward normal vector to the oriented surface $\partial\mathcal{P}$. The referential counterpart $\vec{\varphi}_R(\vec{X},t)$, with $\vec{X} \in \partial\mathcal{P}$, is defined by the identity

$$\int_{\partial\mathcal{P}_t} \vec{\varphi}(\vec{x},t)\cdot\vec{n}\,\mathrm{d}a = \int_{\partial\mathcal{P}} \vec{\varphi}_R(\vec{X},t)\cdot\vec{n}_R\,\mathrm{d}A\ , \tag{4}$$

imposed on all $\partial\mathcal{P}_t \subset \partial\mathcal{B}_t$.

Due to the Nanson's formula for area changes, $\vec{n}\,\mathrm{d}a = J\,\mathbf{F}^{-\mathrm{T}}\,\vec{n}_R\,\mathrm{d}A$, Eq. (4) implies

$$\vec{\varphi}_R(\vec{X},t) = J(\vec{X},t)\,\mathbf{F}^{-1}(\vec{X},t)\,\vec{\varphi}(\vec{x}(\vec{X},t),t). \tag{5}$$

3. Kinematics

Following Anand (2012), we base the theory on the following multiplicative decomposition of the deformation gradient

$$\mathbf{F} = \mathbf{F}^{cte}\,\mathbf{F}^{p}\ , \tag{6}$$

where $\mathbf{F}^{cte}$ is termed chemo-thermo-elastic deformation gradient, and represents the distorsion of the material in the neighborhood of $\vec{X}$ as a consequence of the combined effect of the chemical, temperature dependent and elastic mechanisms; $\mathbf{F}^{p}$ is termed inelastic distorsion and represents the irreversible deformations in the neighborhood of $\vec{X}$ due, for instance, to the flow of defects (Gurtin et al., 2010) in plasticity (see Fig. 2).

The chemo-thermo-elastic deformation gradient $\mathbf{F}^{cte}$ is in turn subject to the further multiplicative decomposition

$$\mathbf{F}^{cte} = \mathbf{F}^{e}\,\mathbf{F}^{th}\,\mathbf{F}^{s}\ , \tag{7}$$

with $\mathbf{F}^{e}$ the local reversible elastic distorsion, $\mathbf{F}^{th}$ the thermal contribution to the local distorsion, and $\mathbf{F}^{s}$ the local distorsion of the material due to volumetric swelling (shrinking) as a consequence of the trapping (extraction) of species in (from) the host material. A similar decomposition of the deformation gradient has been proposed in Serpelloni et al. (2021) and Anand (2012), *although the thermal contribution has not been accounted for*. Bearing in mind the velocity gradient, $\boldsymbol{l} = \dot{\mathbf{F}}\,\mathbf{F}^{-1}$, and according to Eq. (6), the chemo-thermo elastic and the inelastic velocity gradient will be defined by

$$\boldsymbol{l}^{cte} = \dot{\mathbf{F}}^{cte}\,\mathbf{F}^{cte^{-1}}\ , \tag{8a}$$

$$\boldsymbol{l}^{p} = \dot{\mathbf{F}}^{p}\,\mathbf{F}^{p^{-1}}\ , \tag{8b}$$

so that

$$\boldsymbol{l} = \dot{\mathbf{F}}\,\mathbf{F}^{-1} = \boldsymbol{l}^{cte} + \mathbf{F}^{cte}\,\boldsymbol{l}^{p}\,\mathbf{F}^{cte^{-1}}. \tag{9}$$

As standard in continuum mechanics, the decomposition of the velocity gradient into the symmetric stretch tensor $\boldsymbol{d}$ and the skew spin tensor $\boldsymbol{w}$, the chemo-thermo-elastic and the plastic velocity gradients can be expressed as

$$\boldsymbol{l}^{cte} = \boldsymbol{d}^{cte} + \boldsymbol{w}^{cte}, \qquad \boldsymbol{l}^{p} = \boldsymbol{d}^{p} + \boldsymbol{w}^{p}. \tag{10}$$

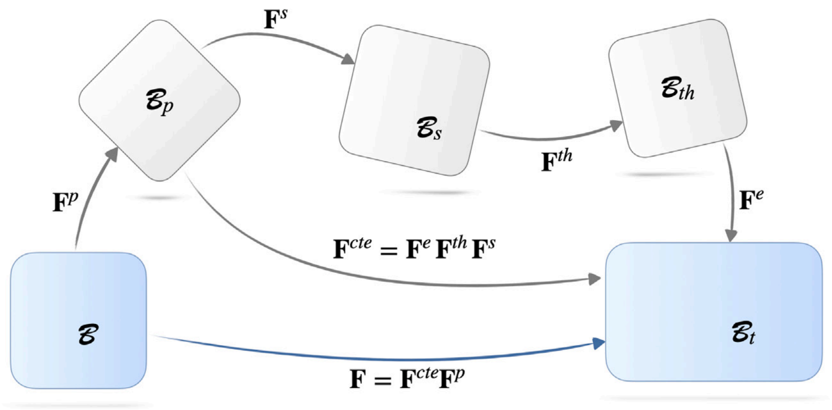

Fig. 2. A schematic of the material $\mathcal{B}$, and spatial $\mathcal{B}_t$ configurations, and of the multiplicative decomposition of the deformation gradient in plasticity $\mathbf{F}^p$, from material to plastic configuration $\mathcal{B}_p$, and chemo-termo-elastic $\mathbf{F}^{cte}$, from plastic to spatial configuration. The further multiplicative decomposition of $\mathbf{F}^{cte}$ entails the swelling contribution $\mathbf{F}^s$, from plastic to swelling $\mathcal{B}_s$, the thermal contribution $\mathbf{F}^{th}$, from swelling to thermal $\mathcal{B}_{th}$, and the elastic contribution $\mathbf{F}^e$, from $\mathcal{B}_{th}$ to $\mathcal{B}_t$.

4. Balance laws

In the present framework, we maintain the same hypothesis assumed in Salvadori et al. (2018b). Only isolated saturable and reversible trap sites are considered, since they are assumed to not form an extended continuous path for lattice species diffusion. For this reason, freely diffusive species through the host lattice network fill trap sites and, once in the trap, cease to diffuse. Species transport is therefore attributed solely to the lattice (interstitial) sites. Hence, the referential flux of species (number of moles of species α measured per unit reference area per unit time), here denoted with $\vec{h}_{\alpha_R}$, only has a purely interstitial lattice diffusion contribution, as in Larche and Cahn (1973, 1978).

4.1. Mass balance

Consider a generic species H at a point $\vec{X} \in \mathcal{P}$. The trapping process of H describes the conversion of mobile species to trapped species, and vice-versa, via the following one-component two-phases chemical reaction

$$\mathrm{H}_L \overset{k_{T_R}}{\underset{k_{L_R}}{\rightleftarrows}} \mathrm{H}_T \, , \tag{11}$$

where k_{T_R} and k_{L_R} represent the referential positive rate factor for the forward reaction, yielding trapped species, and for the backward reaction, yielding free diffusive species, respectively. The reaction rate of Eq. (11) is denoted with $w_R^{(11)}$; specifications of $w_R^{(11)}$, k_{T_R} and k_{L_R} will be provided in Section 7.

Let ρ_{α_R}, c_{α_R} and κ_α denote the referential density (mass per unit reference volume), the referential concentration (moles per unit reference volume) and the molar mass of species α, respectively. The three terms are linked to each other by means of the relation

$$\rho_{\alpha_R} = \kappa_\alpha \, c_{\alpha_R} . \tag{12}$$

Accordingly, mass balance equations for species $\alpha = L, T$ can be formulated either in terms of density or in terms of concentration of species, in the reference configuration:

$$\frac{\mathrm{d}}{\mathrm{d}t} \int_{\mathcal{P}} c_{\alpha_R}(\vec{X},t)\, \mathrm{d}V + \int_{\partial\mathcal{P}} \vec{h}_{\alpha_R}(\vec{X},t) \cdot \vec{n}_R \, \mathrm{d}A \pm \int_{\mathcal{P}} w_R^{(11)}(\vec{X},t)\, \mathrm{d}V = \int_{\mathcal{P}} s_{\alpha_R}(\vec{X},t)\, \mathrm{d}V . \tag{13}$$

The right-hand side term s_{α_R} is the rate, in moles per unit reference volume per unit time, at which species α are generated by external sources, where a positive reaction rate $w_R^{(11)}$ refers to the free species L.

After application of the divergence theorem, Eq. (13) takes the form

$$\int_{\mathcal{P}} \frac{\partial}{\partial t} c_{\alpha_R}(\vec{X},t)\, \mathrm{d}V + \int_{\mathcal{P}} \mathrm{Div}\left[\vec{h}_{\alpha_R}(\vec{X},t) \right] \mathrm{d}V \pm \int_{\mathcal{P}} w_R^{(11)}(\vec{X},t)\, \mathrm{d}V = \int_{\mathcal{P}} s_{\alpha_R}(\vec{X},t)\, \mathrm{d}V \, , \tag{14}$$

for any region $\mathcal{P} \subset \mathcal{B}$.

It follows that, by means of the assumption of immobilized trapped species which therefore provides no mass flux of H_T ($\vec{h}_{T_R} = \vec{0}$), the referential local form of the mass balance equations write as

$$\frac{\partial c_{L_R}}{\partial t} + \mathrm{Div}\left[\vec{h}_{L_R} \right] + w_R^{(11)} = s_{L_R} \, , \tag{15a}$$

$$\frac{\partial c_{T_R}}{\partial t} - w^{(11)}_R = s_{T_R}. \tag{15b}$$

The concentrations c_{α_R}, the reaction rate $w^{(11)}_R$ and the rate at which species are generated by sources s_{α_R}, being defined over a volume, transform according to Eq. (3),

$$c_{\alpha_R}(\vec{X},t) = J\, c_\alpha \ , \qquad w^{(11)}_R(\vec{X},t) = J\, w^{(11)} \ , \qquad s_{\alpha_R}(\vec{X},t) = J\, s_\alpha \ , \tag{16}$$

whereas the mass flux $\vec{h}_{L_R}$ follows the rule stated by Eq. (5), namely,

$$\vec{h}_{L_R}(\vec{X},t) = J\, \mathbf{F}^{-1}\, \vec{h}_L. \tag{17}$$

4.2. *Balance of linear and angular momentum*

Let

$$\vec{t}(\vec{x},t) = \boldsymbol{\sigma}\, \vec{n} \tag{18}$$

define the current surface traction (force per unit current surface), with $\boldsymbol{\sigma}$ the Cauchy stress tensor. By means of the Nanson's formula for the transformation of areas,

$$\int_{\partial\mathcal{P}_t} \vec{t}(\vec{x},t)\, \mathrm{d}a = \int_{\partial\mathcal{P}_t} \boldsymbol{\sigma}(\vec{x},t)\, \vec{n}\, \mathrm{d}a = \int_{\partial\mathcal{P}} \boldsymbol{\sigma}\, J\, \mathbf{F}^{-\mathrm{T}}\, \vec{n}_R\, \mathrm{d}A = \int_{\partial\mathcal{P}} \mathbf{P}(\vec{X},t)\, \vec{n}_R\, \mathrm{d}A = \int_{\partial\mathcal{P}} \vec{t}_R(\vec{X},t)\, \mathrm{d}A \ , \tag{19}$$

with $\vec{t}_R$ the referential surface traction (spatial force with material reference, *i.e.*, traction per unit reference surface Steinmann et al., 2009) and $\mathbf{P}$ the nominal, or first Piola–Kirchhoff, stress tensor, defined as

$$\mathbf{P} = J\, \boldsymbol{\sigma}\, \mathbf{F}^{-\mathrm{T}}. \tag{20}$$

As in Salvadori et al. (2018b), inertia body forces are neglected and this implies that the referential balance of linear momentum takes the form

$$\mathrm{Div}\,[\,\mathbf{P}\,] + \vec{b}^{\,0}_R = \vec{0}\ , \tag{21}$$

where $\vec{b}^{\,0}_R$ represents the referential body force (spatial body force density in the material reference configuration, *i.e.*, body force acting on a unit volume in the material configuration Steinmann et al., 2009), and $\mathrm{Div}\,[\,\mathbf{P}\,] = \partial \mathrm{P}_{ij}/\partial X_j$.

The referential form of the balance of angular momentum writes as

$$\mathbf{P}\,\mathbf{F}^{\mathrm{T}} = \mathbf{F}\,\mathbf{P}^{\mathrm{T}}. \tag{22}$$

5. Thermodynamics

5.1. *Energy balance*

We augment the classical first law of thermodynamics, which provides the variation of the internal energy of a body as the sum of the power expended on it by external forces and the heat transferred in it, with the energy flow due to species transport. The first law of thermodynamics is therefore represented by the interplay among the internal energy of $\mathcal{P}$, the power expended on $\mathcal{P}$, the heat transferred in $\mathcal{P}$, and the power due to mass exchanged on $\mathcal{P}$. Electro-magnetic effects will be accounted for in a forthcoming publication, but are omitted here.

Denote with $\mathcal{U}$ the net internal energy, $\mathcal{W}_u$ the mechanical external power, $\mathcal{Q}_u$ the power due to heat transferred, and $\mathcal{T}_u$ the power due to mass transferred. The referential energy balance takes the form

$$\frac{\mathrm{d}}{\mathrm{d}t}\, \mathcal{U}(\mathcal{P}) = \mathcal{W}_u(\mathcal{P}) + \mathcal{Q}_u(\mathcal{P}) + \mathcal{T}_u(\mathcal{P}). \tag{23}$$

We point out that the assumption of negligible inertia forces implies that no kinetic energy is accounted for; on the same grounds, the mechanical external power is defined in terms of the body forces and surface tractions.

The definition of the referential net internal energy can be provided either per unit reference mass or per unit reference volume, given that the referential mass density does not change in time ($\dot{\rho}_R = 0$) in view of the mass conservation for the hosting material. By defining u_R as the specific internal energy (per unit reference volume), we write the individual contributions of Eq. (23) as

$$\frac{\mathrm{d}}{\mathrm{d}t}\, \mathcal{U}(\mathcal{P}) = \int_{\mathcal{P}} \frac{\mathrm{d}u_R}{\mathrm{d}t}\, \mathrm{d}V \ , \tag{24a}$$

$$\mathcal{W}_u(\mathcal{P}) = \int_{\partial\mathcal{P}} \dot{\vec{\chi}} \cdot \vec{t}_R\, \mathrm{d}A + \int_{\mathcal{P}} \dot{\vec{\chi}} \cdot \vec{b}^{\,0}_R\, \mathrm{d}V \ , \tag{24b}$$

$$\mathcal{Q}_u(\mathcal{P}) = \int_{\mathcal{P}} s_{q\,R}\, \mathrm{d}V - \int_{\partial\mathcal{P}} \vec{q}_R \cdot \vec{n}_R\, \mathrm{d}A \ , \tag{24c}$$

$$\mathcal{T}_u(\mathcal{P}) = \int_{\mathcal{P}} {}^{u}\mu_L\, s_{L_R} + {}^{u}\mu_T\, s_{T_R}\, \mathrm{d}V - \int_{\partial\mathcal{P}} {}^{u}\mu_L\, \vec{h}_{L_R} \cdot \vec{n}_R\, \mathrm{d}A. \tag{24d}$$

Terms in Eqs. (24) have the following meaning: the surface traction and the body force, $\vec{t}_R$ and $\vec{b}^0_R$, have been defined in Section 4.2; $s_{q\,R}$ and $\vec{q}_R$ represent the heat supplied by external agencies and the heat flux vector, respectively; the scalar ${}^u\mu_\alpha$ is the energy provided by a unit supply of moles of species $\alpha = L, T$, whereas s_{α_R} and $\vec{h}_{L_R}$ are the source term and the mass flux vector, respectively, as defined in the mass balance Eq. (13).

In view of the definition of the referential surface traction arising from Eq. (19), the power expenditure of external agencies $\mathcal{W}_u$ becomes

$$\mathcal{W}_u(\mathcal{P}) = \int_{\mathcal{P}} \mathbf{P} : \dot{\mathbf{F}} \, \mathrm{d}V \,, \tag{25}$$

according to the balance of linear momentum (21).

Application of the divergence theorem to the second term on the right-hand side of Eq. (24c) allows us to write the heat contribution to the energy balance as

$$\mathcal{Q}_u(\mathcal{P}) = \int_{\mathcal{P}} s_{q\,R} - \mathrm{Div}\left[\, \vec{q}_R \,\right] \, \mathrm{d}V \tag{26}$$

where $s_{q\,R}$ and $\vec{q}_R$ follow the transformation rules given by Eqs. (3) and (5), respectively.

The mass transfer contribution to the energy balance, after application of the divergence theorem and use of the localized mass balance Eqs. (15) to substitute for the terms s_{L_R} and s_{T_R}, writes as

$$\begin{aligned} \mathcal{T}_u(\mathcal{P}) &= \int_{\mathcal{P}} {}^u\mu_L \, s_{L_R} + {}^u\mu_T \, s_{T_R} - \mathrm{Div}\left[{}^u\mu_L \, \vec{h}_{L_R} \right] \, \mathrm{d}V \\ &= \int_{\mathcal{P}} {}^u\mu_L \, \frac{\partial c_{L_R}}{\partial t} + {}^u\mu_T \, \frac{\partial c_{T_R}}{\partial t} - \mathrm{Grad}\left[{}^u\mu_L \right] \cdot \vec{h}_{L_R} + \left({}^u\mu_L - {}^u\mu_T \right) w_R^{(11)} \, \mathrm{d}V . \end{aligned} \tag{27}$$

Combining Eqs. (24a), (25), (26) and (27), we find that the referential form of the energy balance writes as

$$\begin{aligned} \int_{\mathcal{P}} \frac{\mathrm{d}u_R}{\mathrm{d}t} \, \mathrm{d}V = \int_{\mathcal{P}} & \mathbf{P} : \dot{\mathbf{F}} + s_{q\,R} - \mathrm{Div}\left[\, \vec{q}_R \,\right] + {}^u\mu_L \, \frac{\partial c_{L_R}}{\partial t} - \vec{h}_{L_R} \cdot \mathrm{Grad}\left[{}^u\mu_L \right] + {}^u\mu_T \, \frac{\partial c_{T_R}}{\partial t} \\ & + \left({}^u\mu_L - {}^u\mu_T \right) \, w_R^{(11)} \, \mathrm{d}V . \end{aligned} \tag{28}$$

Since it must hold for any arbitrary region $\mathcal{P} \subset \mathcal{B}$, Eq. (28) can be localized as

$$\frac{\mathrm{d}u_R}{\mathrm{d}t} = \mathbf{P} : \dot{\mathbf{F}} + s_{q\,R} - \mathrm{Div}\left[\, \vec{q}_R \,\right] + {}^u\mu_L \, \frac{\partial c_{L_R}}{\partial t} - \vec{h}_{L_R} \cdot \mathrm{Grad}\left[{}^u\mu_L \right] + {}^u\mu_T \, \frac{\partial c_{T_R}}{\partial t} + \left({}^u\mu_L - {}^u\mu_T \right) \, w_R^{(11)} . \tag{29}$$

5.2. Entropy imbalance

Similarly to the energy balance, we augment the second law of thermodynamics with a flux of entropy due to species transport. We further assume that the mechanics does not contribute directly to the total entropy flow (Tadmor et al., 2011; De Groot and Mazur, 1984). The second law of thermodynamics is therefore defined as the balance of the interplay among the internal entropy of $\mathcal{P}$ and the entropy transferred in $\mathcal{P}$ due to the mass and the heat transferred on $\mathcal{P}$.

Denote with $\mathcal{S}$ the net internal entropy of $\mathcal{P}$, with $\mathcal{S}_i$ the entropy produced inside $\mathcal{P}$, with $\mathcal{Q}_\eta$ and $\mathcal{T}_\eta$ the entropy per unit time due to the heat and mass transfer, respectively. Then

$$\frac{\mathrm{d}}{\mathrm{d}t} \, \mathcal{S}(\mathcal{P}) - \frac{\mathrm{d}}{\mathrm{d}t} \, \mathcal{S}_i(\mathcal{P}) = \mathcal{Q}_\eta(\mathcal{P}) + \mathcal{T}_\eta(\mathcal{P}) \,, \tag{30}$$

The second law of thermodynamics states

$$\frac{\mathrm{d}}{\mathrm{d}t} \, \mathcal{S}_i(\mathcal{P}) \geq 0 \,, \tag{31}$$

from which Eq. (30) can be re-written in the form

$$\frac{\mathrm{d}}{\mathrm{d}t} \, \mathcal{S}(\mathcal{P}) - \mathcal{Q}_\eta(\mathcal{P}) - \mathcal{T}_\eta(\mathcal{P}) \geq 0. \tag{32}$$

We state the specific net internal entropy (per unit reference volume) η_R so that the individual contributions of the entropy imbalance (32) write as

$$\frac{\mathrm{d}}{\mathrm{d}t} \, \mathcal{S}(\mathcal{P}) = \int_{\mathcal{P}} \frac{\mathrm{d}\eta_R}{\mathrm{d}t} \, \mathrm{d}V \,, \tag{33a}$$

$$\mathcal{Q}_\eta(\mathcal{P}) = \int_{\mathcal{P}} \frac{1}{T} \, s_{q\,R} \, \mathrm{d}V - \int_{\partial\mathcal{P}} \frac{1}{T} \, \vec{q}_R \cdot \vec{n}_R \, \mathrm{d}A \,, \tag{33b}$$

$$\mathcal{T}_\eta(\mathcal{P}) = \int_{\mathcal{P}} {}^\eta\mu_L \, s_{L_R} + {}^\eta\mu_T \, s_{T_R} \, \mathrm{d}V - \int_{\partial\mathcal{P}} {}^\eta\mu_L \, \vec{h}_{L_R} \cdot \vec{n}_R \, \mathrm{d}A \,, \tag{33c}$$

with ${}^\eta\mu_\alpha$ the change in specific entropy provided by a unit supply of moles of species $\alpha = L, T$.

Application of the divergence theorem leads to

$$\mathcal{Q}_\eta(\mathcal{P}) = \int_{\mathcal{P}} \frac{1}{T} \, s_{q\,R} - \mathrm{Div}\left[\frac{1}{T} \, \vec{q}_R \right] \, \mathrm{d}V = \int_{\mathcal{P}} \frac{1}{T} \, s_{q\,R} - \frac{1}{T} \, \mathrm{Div}\left[\, \vec{q}_R \,\right] + \frac{1}{T^2} \, \vec{q}_R \cdot \mathrm{Grad}\left[\, T \,\right] \, \mathrm{d}V \,, \tag{34}$$

and the procedure performed to derive the mass contribution to the energy balance $\mathcal{T}_u(\mathcal{P})$ given by Eq. (27) allows us to write

$$\mathcal{T}_\eta(\mathcal{P}) = \int_{\mathcal{P}} {}^\eta\mu_L \, \frac{\partial c_{L_R}}{\partial t} + {}^\eta\mu_T \, \frac{\partial c_{T_R}}{\partial t} - \mathrm{Grad}\left[{}^\eta\mu_L \right] \cdot \vec{h}_{L_R} + \left({}^\eta\mu_L - {}^\eta\mu_T \right) w_R^{(11)} \, \mathrm{d}V . \tag{35}$$

Eventually, the second law of thermodynamics can be stated as

$$\begin{aligned} \int_{\mathcal{P}} \frac{\mathrm{d}\eta_R}{\mathrm{d}t} \, \mathrm{d}V - \int_{\mathcal{P}} \frac{1}{T} \, s_{q\,R} - \frac{1}{T} \, \mathrm{Div}\left[\vec{q}_R \right] + \frac{1}{T^2} \, \vec{q}_R \cdot \mathrm{Grad}\left[T \right] \, \mathrm{d}V - \int_{\mathcal{P}} {}^\eta\mu_L \, \frac{\partial c_{L_R}}{\partial t} + {}^\eta\mu_T \, \frac{\partial c_{T_R}}{\partial t} \\ - \vec{h}_{L_R} \cdot \mathrm{Grad}\left[{}^\eta\mu_L \right] + \left({}^\eta\mu_L - {}^\eta\mu_T \right) w_R^{(11)} \, \mathrm{d}V \geq 0 \, , \end{aligned} \tag{36}$$

on any arbitrary region $\mathcal{P} \subset \mathcal{B}$. Eq. (36) can be localized as

$$\begin{aligned} T \, \frac{\mathrm{d}\eta_R}{\mathrm{d}t} - s_{q\,R} + \mathrm{Div}\left[\vec{q}_R \right] - \frac{1}{T} \, \vec{q}_R \cdot \mathrm{Grad}\left[T \right] - T \, {}^\eta\mu_L \, \frac{\partial c_{L_R}}{\partial t} - T \, {}^\eta\mu_T \, \frac{\partial c_{T_R}}{\partial t} + T \, \vec{h}_{L_R} \cdot \mathrm{Grad}\left[{}^\eta\mu_L \right] \\ - T \, \left({}^\eta\mu_L - {}^\eta\mu_T \right) \, w_R^{(11)} \geq 0 \, , \end{aligned} \tag{37}$$

after multiplication by the temperature.

Taking advantage of Eq. (29) to replace the factor $-s_{q\,R} + \mathrm{Div}\left[\vec{q}_R \right]$ in Eq. (37), we can rephrase the second law of thermodynamics as

$$\begin{aligned} T \, \frac{\mathrm{d}\eta_R}{\mathrm{d}t} - \frac{\mathrm{d}u_R}{\mathrm{d}t} + \mathbf{P} : \dot{\mathbf{F}} + \left({}^u\mu_L - T \, {}^\eta\mu_L \right) \, \frac{\partial c_{L_R}}{\partial t} + \left({}^u\mu_T - T \, {}^\eta\mu_T \right) \, \frac{\partial c_{T_R}}{\partial t} - \vec{h}_{L_R} \cdot \mathrm{Grad}\left[{}^u\mu_L \right] \\ - \frac{1}{T} \, \vec{q}_R \cdot \mathrm{Grad}\left[T \right] + T \, \vec{h}_{L_R} \cdot \mathrm{Grad}\left[{}^\eta\mu_L \right] + \left({}^u\mu_L - T \, {}^\eta\mu_L \right) \, w_R^{(11)} - \left({}^u\mu_T - T \, {}^\eta\mu_T \right) \, w_R^{(11)} \geq 0. \end{aligned} \tag{38}$$

By denoting

$$\mu_\alpha = {}^u\mu_\alpha - T \, {}^\eta\mu_\alpha \, , \tag{39}$$

$$A^{(11)} = \mu_T - \mu_L \, , \tag{40}$$

we can cast the entropy imbalance (38) in the form

$$\begin{aligned} T \, \frac{\mathrm{d}\eta_R}{\mathrm{d}t} - \frac{\mathrm{d}u_R}{\mathrm{d}t} + \mathbf{P} : \dot{\mathbf{F}} + \mu_L \, \frac{\partial c_{L_R}}{\partial t} + \mu_T \, \frac{\partial c_{T_R}}{\partial t} - \vec{h}_{L_R} \cdot \mathrm{Grad}\left[{}^u\mu_L \right] - \frac{1}{T} \, \vec{q}_R \cdot \mathrm{Grad}\left[T \right] \\ + T \, \vec{h}_{L_R} \cdot \mathrm{Grad}\left[{}^\eta\mu_L \right] - A^{(11)} \, w_R^{(11)} \geq 0. \end{aligned} \tag{41}$$

Following Salvadori et al. (2018b), we introduce a new referential heat flux as

$$\vec{\not{q}}_R = \vec{q}_R + T \, {}^\eta\mu_L \, \vec{h}_{L_R} \, , \tag{42}$$

which leads to the alternative localized referential form of the entropy imbalance

$$T \, \frac{\mathrm{d}\eta_R}{\mathrm{d}t} - \frac{\mathrm{d}u_R}{\mathrm{d}t} + \mathbf{P} : \dot{\mathbf{F}} - \frac{1}{T} \, \vec{\not{q}}_R \cdot \mathrm{Grad}\left[T \right] + \mu_L \, \frac{\partial c_{L_R}}{\partial t} + \mu_T \, \frac{\partial c_{T_R}}{\partial t} - \vec{h}_{L_R} \cdot \mathrm{grad}\left[\mu_L \right] - A^{(11)} \, w_R^{(11)} \geq 0. \tag{43}$$

5.2.1. Stress measures

The multiplicative decomposition of the deformation gradient performed in Eq. (6) leads to the splitting of the mechanical contribution to the entropy imbalance (43) into two separate terms, following the same path of reasoning of Anand (2012).

By means of Eq. (6), and the definition of the first Piola–Kirchhoff stress tensor (20), it holds that

$$\mathbf{P} : \dot{\mathbf{F}} = J \, \boldsymbol{\sigma} \, \mathbf{F}^{-\mathrm{T}} : \dot{\mathbf{F}} = J \, \boldsymbol{\sigma} \, \mathbf{F}^{cte^{-\mathrm{T}}} \, \mathbf{F}^{p^{-\mathrm{T}}} : \dot{\mathbf{F}}^{cte} \, \mathbf{F}^{p} + J \, \boldsymbol{\sigma} \, \mathbf{F}^{cte^{-\mathrm{T}}} \, \mathbf{F}^{p^{-\mathrm{T}}} : \mathbf{F}^{cte} \, \dot{\mathbf{F}}^{p}. \tag{44}$$

The first term on the right-hand side of Eq. (44) can be manipulated in order to obtain

$$J \, \boldsymbol{\sigma} \, \mathbf{F}^{cte^{-\mathrm{T}}} \, \mathbf{F}^{p^{-\mathrm{T}}} : \dot{\mathbf{F}}^{cte} \, \mathbf{F}^{p} = J^{cte} \, J^{p} \, \boldsymbol{\sigma} \, \mathbf{F}^{cte^{-\mathrm{T}}} : \dot{\mathbf{F}}^{cte} = J^{p} \, \mathbf{P}^{cte} : \dot{\mathbf{F}}^{cte} \tag{45}$$

which represents the chemo-thermo-elastic part of the mechanical contribution to the entropy imbalance, and where the chemo-thermo-elastic first Piola–Kirchhoff stress tensor is defined as

$$\mathbf{P}^{cte} = J^{cte} \, \boldsymbol{\sigma} \, \mathbf{F}^{cte^{-\mathrm{T}}} . \tag{46}$$

Another stress measure commonly used in finite strain theory in continuum mechanics is the second Piola–Kirchhoff stress tensor, here denoted with $\mathbf{S}$ and related to the first Piola–Kirchhoff stress tensor via the standard relation $\mathbf{P} = \mathbf{F}\,\mathbf{S}$. It is therefore possible to define the chemo-thermo-elastic second Piola–Kirchhoff stress tensor $\mathbf{S}^{cte}$ as

$$\mathbf{S}^{cte} = \mathbf{F}^{cte^{-1}} \, \mathbf{P}^{cte} = J^{cte} \, \mathbf{F}^{cte^{-1}} \, \boldsymbol{\sigma} \, \mathbf{F}^{cte^{-\mathrm{T}}} \, , \tag{47}$$

whence, Eq. (45) can be cast in the form

$$J^{p} \, \mathbf{P}^{cte} : \dot{\mathbf{F}}^{cte} = J^{p} \, \mathbf{S}^{cte} : \dot{\mathbf{E}}^{cte} = J^{p} \, \mathbf{S}^{cte} : \frac{1}{2} \, \dot{\mathbf{C}}^{cte} \, . \tag{48}$$

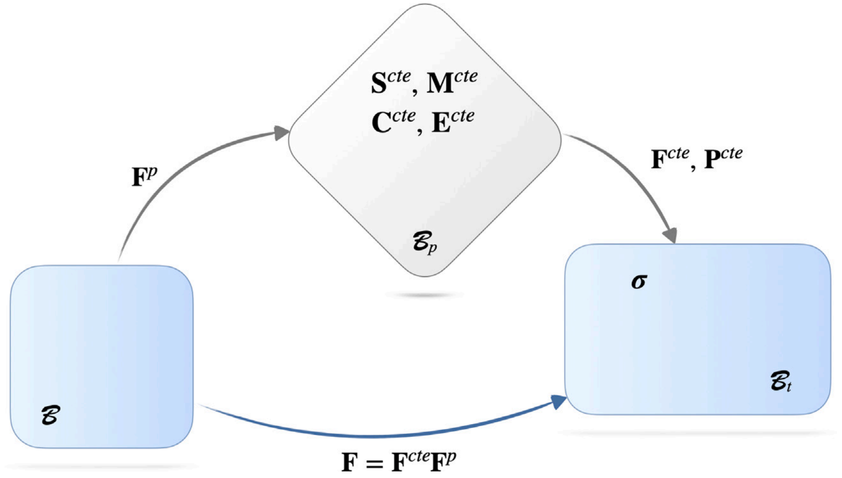

Fig. 3. Schematic of the material $\mathcal{B}$, intermediate $\mathcal{B}_p$, and spatial $\mathcal{B}_t$ configurations, and of the stress and strain tensors in their domains. The chemo-thermo-elastic second Piola–Kirchhoff and Mandel stress tensors, $\mathbf{S}^{cte}$ and $\mathbf{M}^{cte}$, the chemo-thermo-elastic right Cauchy–Green and Green–Lagrange strain tensors, $\mathbf{C}^{cte}$ and $\mathbf{E}^{cte}$, from intermediate $\mathcal{B}_p$; the chemo-thermo-elastic first Piola–Kirchhoff stress tensor $\mathbf{P}^{cte}$, from intermediate $\mathcal{B}_p$ to spatial $\mathcal{B}_t$; the Cauchy stress tensor $\boldsymbol{\sigma}$ from spatial $\mathcal{B}_t$.

The chemo-thermo-elastic right Cauchy–Green and Green–Lagrange strain tensors have been defined as

$$\mathbf{C}^{cte} = \mathbf{F}^{cte^{\mathrm{T}}}\mathbf{F}^{cte} \,, \tag{49a}$$

$$\mathbf{E}^{cte} = \frac{1}{2}\left(\mathbf{C}^{cte} - \mathbf{1}\right) . \tag{49b}$$

The second right-hand side term of Eq. (44) represents the inelastic contribution to the entropy imbalance (43), and can be re-written as

$$J\,\boldsymbol{\sigma}\,\mathbf{F}^{cte^{-\mathrm{T}}}\,\mathbf{F}^{p^{-\mathrm{T}}} : \mathbf{F}^{cte}\,\dot{\mathbf{F}}^{p} = J^{cte}\,J^{p}\,\mathbf{F}^{cte^{\mathrm{T}}}\,\boldsymbol{\sigma}\,\mathbf{F}^{cte^{-\mathrm{T}}} : \dot{\mathbf{F}}^{p}\,\mathbf{F}^{p^{-1}} = J^{p}\,\mathbf{M}^{cte} : \boldsymbol{l}^{p} \,, \tag{50}$$

with $\mathbf{M}^{cte}$ chemo-thermo-elastic Mandel stress tensor,

$$\mathbf{M}^{cte} = J^{cte}\,\mathbf{F}^{cte^{\mathrm{T}}}\,\boldsymbol{\sigma}\,\mathbf{F}^{cte^{-\mathrm{T}}} = \mathbf{C}^{cte}\,\mathbf{S}^{cte} \,, \tag{51}$$

according to Eqs. (47), (49a).

Combining Eq. (48) with Eq. (50), we find that the mechanical contribution to the second law of thermodynamics takes the following final form (see Fig. 3)

$$\mathbf{P} : \dot{\mathbf{F}} = J^{p}\,\frac{1}{2}\,\mathbf{S}^{cte} : \dot{\mathbf{C}}^{cte} + J^{p}\,\mathbf{M}^{cte} : \boldsymbol{l}^{p}. \tag{52}$$

5.3. Clausius-Duhem inequality

From the definition of the Helmholtz free energy density (per unit referential volume),

$$\psi_R = u_R - T\,\eta_R \,, \tag{53}$$

the first two terms of the localized referential form of the entropy imbalance (43) can be re-written as

$$T\,\frac{\mathrm{d}\eta_R}{\mathrm{d}t} - \frac{\mathrm{d}u_R}{\mathrm{d}t} = -\frac{\mathrm{d}\psi_R}{\mathrm{d}t} - \frac{\partial T}{\partial t}\,\eta_R. \tag{54}$$

We take the referential Helmholtz free energy density as a function of temperature T, concentrations of species c_{α_R}, chemo-thermo-elastic right Cauchy–Green strain tensor $\mathbf{C}^{cte}$, and of a kinematic tensorial internal variable ξ having the usual meaning in inelastic constitutive laws (Gurtin et al., 2010; Tadmor et al., 2011; Paolucci, 2016; Holzapfel, 2001; Simo, 1988a,b)

$$\psi_R = \psi_R\left(T, c_{L_R}, c_{T_R}, \mathbf{C}^{cte}, \xi\right). \tag{55}$$

The selection of $\mathbf{C}^{cte}$ as the strain internal variable appears here to be the most suitable choice in view of the multiplicative decomposition of the deformation gradient (6), which underpins the proposed framework. It is worth pointing out that alternative choices for the strain could be taken. A suitable choice is represented by the total right Cauchy–Green tensor, since the mechanical contribution in the Clausius-Duhem inequality would be solely represented in terms of total stress and strain tensors, *e.g.*, $\frac{1}{2}\,\mathbf{S} : \dot{\mathbf{C}}$, by following the same path of reasoning which led to Eq. (48).

In view of the selected functional dependence of the referential Helmholtz free energy density shown in Eq. (55), the time derivative of ψ_R writes as

$$\frac{\mathrm{d}\psi_R}{\mathrm{d}t} = \frac{\partial \psi_R}{\partial \mathbf{C}^{cte}} : \frac{\partial \mathbf{C}^{cte}}{\partial t} + \frac{\partial \psi_R}{\partial c_{L_R}} \frac{\partial c_{L_R}}{\partial t} + \frac{\partial \psi_R}{\partial c_{T_R}} \frac{\partial c_{T_R}}{\partial t} + \frac{\partial \psi_R}{\partial T} \frac{\partial T}{\partial t} + \frac{\partial \psi_R}{\partial \xi} : \frac{\partial \xi}{\partial t} . \tag{56}$$

By denoting the inelastic stress tensor conjugate to ξ as

$$\chi = - \frac{\partial \psi_R}{\partial \xi} \, , \tag{57}$$

we are able to combine Eqs. (43), (52), (56), (57) in the Clausius-Duhem inequality in the form

$$\begin{aligned} \left(\frac{1}{2} \, J^p \, \mathbf{S}^{cte} - \frac{\partial \psi_R}{\partial \mathbf{C}^{cte}} \right) : \frac{\partial \mathbf{C}^{cte}}{\partial t} + \left(\mu_L - \frac{\partial \psi_R}{\partial c_{L_R}} \right) \frac{\partial c_{L_R}}{\partial t} + \left(\mu_T - \frac{\partial \psi_R}{\partial c_{T_R}} \right) \frac{\partial c_{T_R}}{\partial t} - \left(\eta_R + \frac{\partial \psi_R}{\partial T} \right) \frac{\partial T}{\partial t} \\ + \chi : \frac{\partial \xi}{\partial t} + J^p \, \mathbf{M}^{cte} : \boldsymbol{l}^p - \frac{1}{T} \vec{q}_R \cdot \mathrm{Grad}\,[\, T \,] - \vec{h}_{L_R} \cdot \mathrm{Grad}\left[\, \mu_L \,\right] - A^{(11)} \, w_R^{(11)} \geq 0. \end{aligned} \tag{58}$$

This inequality must hold for any value of the time derivative of the strain tensor $\mathbf{C}^{cte}$, of the concentrations of lattice and trapped species c_{L_R} and c_{T_R}, and of the temperature T.

The following thermodynamic restrictions thus arise

$$\mathbf{S}^{cte} = 2 \, J^{p^{-1}} \, \frac{\partial \psi_R}{\partial \mathbf{C}^{cte}} \bigg|_{T, c_{L_R}, c_{T_R}, \xi} \, , \tag{59a}$$

$$\eta_R = - \frac{\partial \psi_R}{\partial T} \bigg|_{c_{L_R}, c_{T_R}, \mathbf{C}^{cte}, \xi} \, , \tag{59b}$$

$$\mu_L = \frac{\partial \psi_R}{\partial c_{L_R}} \bigg|_{T, c_{T_R}, \mathbf{C}^{cte}, \xi} \, , \tag{59c}$$

$$\mu_T = \frac{\partial \psi_R}{\partial c_{T_R}} \bigg|_{T, c_{L_R}, \mathbf{C}^{cte}, \xi} \, . \tag{59d}$$

What remains of the Clausius-Duhem inequality (58) establishes irreversible processes. As we cannot place any restriction on the values of $\mathbf{C}^{cte}$, c_{α_R}, and T, the same applies for $\boldsymbol{l}^p$, ξ, $\mathrm{Grad}\left[\, \mu_L \,\right]$, $\mathrm{Grad}\,[\, T \,]$, and $w_R^{(11)}$. As a consequence, restrictions on χ, $\mathbf{M}^{cte}$, $\vec{h}_{L_R}$, $\vec{q}_R$, and $A^{(11)}$ are determined. The internal entropy production (multiplied by T), can be written with the usual dissipative structure (Prigogine, 1977), namely

$$\underbrace{J^p \, \mathbf{M}^{cte} : \boldsymbol{l}^p + \chi : \frac{\partial \xi}{\partial t}}_{\text{inelastic}} \underbrace{- \vec{h}_{L_R} \cdot \mathrm{Grad}\left[\, \mu_L \,\right]}_{\text{diffusive}} \underbrace{- \frac{1}{T} \vec{q}_R \cdot \mathrm{Grad}\,[\, T \,]}_{\text{thermal}} \underbrace{- w_R^{(11)} \, A^{(11)}}_{\text{chemical}} \geq 0. \tag{60}$$

No coupling between fluxes and thermodynamic forces of different tensorial order is imposed in view of the assumption of Curie's symmetry principles (De Groot and Mazur, 1984). Therefore the following three conditions arise from the internal entropy production (60)

$$J^p \, \mathbf{M}^{cte} : \boldsymbol{l}^p + \chi : \frac{\partial \xi}{\partial t} \geq 0 \, , \tag{61a}$$

$$\vec{h}_{L_R} \cdot \mathrm{Grad}\left[\, \mu_L \,\right] + \frac{1}{T} \vec{q}_R \cdot \mathrm{Grad}\,[\, T \,] \leq 0 \, , \tag{61b}$$

$$w_R^{(11)} \, A^{(11)} \leq 0 \, . \tag{61c}$$

Inequalities (61) restrict the values that thermodynamic fluxes can assume.

In view of thermodynamic restrictions (59c), (59d), the scalars μ_α declared in Eq. (39) are seen to be chemical potentials, whereas $A^{(11)}$ is the affinity of the chemical reaction (11).

5.4. *Specifications for ${}^{u}\mu_\alpha$ and ${}^{\eta}\mu_\alpha$*

We compute the entropy per mole ${}^{\eta}\mu_\alpha$ as

$${}^{\eta}\mu_\alpha = \frac{\partial \eta_R}{\partial c_{\alpha_R}} \bigg|_{T, \mathbf{C}^{cte}, \xi} = - \frac{\partial^2 \psi_R}{\partial c_{\alpha_R} \partial T} . \tag{62a}$$

According to Eqs. (39), (59c), (59d) and (62a), the energy per mole writes as

$${}^{u}\mu_\alpha = \frac{\partial \psi_R}{\partial c_{\alpha_R}} - T \, \frac{\partial^2 \psi_R}{\partial c_{\alpha_R} \partial T} . \tag{62b}$$

Remark. The identifications of the energetic and entropic contributions to the chemical potential given by Eqs. (62) provide a neat formulation for the entropy production inequality (61b). Recalling the definition of the new referential heat flux $\vec{\not{q}}_R$ (42), we find that

$$\vec{h}_{L_R} \cdot \text{Grad}\left[\mu_L\right] + \frac{1}{T}\vec{\not{q}}_R \cdot \text{Grad}\left[T\right] = \vec{h}_{L_R} \cdot \left(\text{Grad}\left[\mu_L\right] + {}^{\eta}\mu_L \, \text{Grad}\left[T\right]\right) + \frac{1}{T}\vec{q}_R \cdot \text{Grad}\left[T\right] . \tag{63}$$

In addition, Eq. (62a) establishes the independence of the vector $\text{Grad}\left[\mu_L\right] + {}^{\eta}\mu_L \, \text{Grad}\left[T\right]$ from the temperature gradient. Indeed, simple algebra collected in Appendix A.1 leads to

$$\begin{aligned} \text{Grad}\left[\mu_L\right] + {}^{\eta}\mu_L \, \text{Grad}\left[T\right] = {} & \frac{\partial^2 \psi_R}{\partial c_{L_R}^2} \text{Grad}\left[c_{L_R}\right] + \frac{\partial^2 \psi_R}{\partial c_{L_R} \partial c_{T_R}} \text{Grad}\left[c_{T_R}\right] + \frac{\partial^2 \psi_R}{\partial c_{L_R} \partial \mathbf{C}^{cte}} : \text{Grad}\left[\mathbf{C}^{cte}\right] \\ & + \frac{\partial^2 \psi_R}{\partial c_{L_R} \partial \xi} : \text{Grad}\left[\xi\right] . \end{aligned} \tag{64}$$

5.5. *Strain decomposition*

The current Section provides the specifications for both the swelling (de-swelling) contribution and the thermal contribution to the deformation gradient, and the resulting velocity gradients, as performed in Serpelloni et al. (2021) to describe the chemo-thermo-mechanics of cells, and following the path of reasoning of Anand (2012).

Recall the multiplicative decomposition of the $\mathbf{F}^{cte}$ given by Eq. (7). The swelling (de-swelling) distorsion $\mathbf{F}^s$ due to the conversion of mobile to trapped species (and vice-versa), and the thermal distorsion $\mathbf{F}^{th}$, are henceforth assumed to have a spherical form, hence

$$\mathbf{F}^s = \lambda_s \, \mathbf{1} \, , \tag{65a}$$

$$\mathbf{F}^{th} = \lambda_{th} \, \mathbf{1} \, , \tag{65b}$$

with λ_s and λ_{th} positive coefficients termed chemical swelling and thermal stretch, respectively.

The swelling volumetric Jacobian and its evolution in time write as

$$J^s = \det\left[\mathbf{F}^s\right] = \lambda_s^3 \, , \tag{66a}$$

$$\dot{J}^s = 3 \, \lambda_s^2 \, \dot{\lambda}_s \, , \tag{66b}$$

and the velocity gradient

$$\boldsymbol{l}^s = \dot{\mathbf{F}}^s \, \mathbf{F}^{s^{-1}} = \frac{\dot{\lambda}_s}{\lambda_s} \mathbf{1} = \frac{1}{\lambda_s} \frac{1}{3} \frac{\dot{J}_s}{\lambda_s^2} \mathbf{1} = \frac{1}{3} \frac{\dot{J}_s}{\lambda_s^3} \mathbf{1} = \frac{1}{3} \frac{\dot{J}^s}{J^s} \mathbf{1}. \tag{67}$$

Having the same spherical form of $\mathbf{F}^s$, the thermal distorsion $\mathbf{F}^{th}$, given by Eq. (65b), leads to results of the same form. Hence, with regard to the thermal volumetric Jacobian, it holds

$$J^{th} = \det\left[\mathbf{F}^{th}\right] = \lambda_{th}^3 \, , \tag{68a}$$

$$\dot{J}^{th} = 3 \, \lambda_{th}^2 \, \dot{\lambda}_{th} \, , \tag{68b}$$

whereas the thermal velocity gradient writes as

$$\boldsymbol{l}^{th} = \dot{\mathbf{F}}^{th} \, \mathbf{F}^{th^{-1}} = \frac{\dot{\lambda}_{th}}{\lambda_{th}} \mathbf{1} = \frac{1}{3} \frac{\dot{J}^{th}}{J^{th}} \mathbf{1}. \tag{69}$$

We further assume that the skew-symmetric part of both the swelling velocity gradient and the thermal velocity gradient are negligible, therefore $\boldsymbol{w}^s = 0$ and $\boldsymbol{w}^{th} = 0$, from which descends

$$\boldsymbol{l}^s \equiv \boldsymbol{d}^s \, , \qquad \boldsymbol{l}^{th} \equiv \boldsymbol{d}^{th}. \tag{70}$$

5.5.1. *Assumptions on $\boldsymbol{l}^s$*

To specify the swelling velocity gradient (67) in terms of concentrations of diffusive and trapped species, c_{L_R} and c_{T_R}, take a function $f^s(c_{L_R}, c_{T_R})$, and define the swelling volumetric Jacobian as

$$J^s = f^s(c_{L_R}, c_{T_R}) = f_L^s(c_{L_R}) \, f_T^s(c_{T_R}). \tag{71}$$

Furthermore, denote with $\omega_L^s > 0$ and $\omega_T^s > 0$ the chemical expansion coefficients of species L and T, obtained as the derivative of Eq. (71) with respect to c_{L_R} and c_{T_R}, respectively. Then

$$\omega_L^s(c_{L_R}, c_{T_R}) = \frac{\partial f_L^s(c_{L_R})}{\partial c_{L_R}} \, f_T^s(c_{T_R}) \, , \tag{72a}$$

$$\omega_T^s(c_{L_R}, c_{T_R}) = \frac{\partial f_T^s(c_{T_R})}{\partial c_{T_R}} \, f_T^s(c_{L_R}). \tag{72b}$$

According to Eqs. (72), the evolution in time of J^s (71) can be re-written as

$$\dot{J}^s = \dot{f}^s(c_{L_R}, c_{T_R}) = \omega^s_L \, \frac{\partial c_{L_R}}{\partial t} + \omega^s_T \, \frac{\partial c_{T_R}}{\partial t} . \tag{73}$$

Denote with Θ^s_L, Θ^s_T the ratio between Eqs. (72a), (72b) and Eq. (71), namely

$$\Theta^s_L(c_{L_R}) = \frac{\omega^s_L(c_{L_R}, c_{T_R})}{f^s(c_{L_R}, c_{T_R})} = \frac{1}{f^s_L(c_{L_R}) \, f^s_T(c_{T_R})} \, \frac{\partial f^s_{L_R}}{\partial c_{L_R}} \, f^s_T(c_{T_R}) = \frac{1}{f^s_L} \, \frac{\partial f^s_{L_R}}{\partial c_{L_R}} \, , \tag{74a}$$

$$\Theta^s_T(c_{T_R}) = \frac{\omega^s_T(c_{L_R}, c_{T_R})}{f^s(c_{L_R}, c_{T_R})} = \frac{1}{f^s_L(c_{L_R}) \, f^s_T(c_{T_R})} \, \frac{\partial f^s_{T_R}}{\partial c_{T_R}} \, f^s_L(c_{L_R}) = \frac{1}{f^s_T} \, \frac{\partial f^s_{T_R}}{\partial c_{T_R}} . \tag{74b}$$

Simple algebra allows us to write the swelling velocity gradient $\boldsymbol{l}^s$ in the form

$$\boldsymbol{l}^s = \frac{1}{3} \, \frac{\dot{J}^s}{J^s} \, \mathbf{1} = \frac{1}{3} \left(\Theta^s_L \, \frac{\partial c_{L_R}}{\partial t} + \Theta^s_T \, \frac{\partial c_{T_R}}{\partial t} \right) \mathbf{1}. \tag{75}$$

A classical specification for the functions $f^s_L(c_{L_R})$ and $f^s_T(c_{T_R})$ is represented by the relations

$$f^s_L(c_{L_R}) = 1 + \left(c_{L_R} - c^0_{L_R} \right) \, \omega^s_{L_R} \, , \qquad f^s_T(c_{T_R}) = 1 + \left(c_{T_R} - c^0_{T_R} \right) \, \omega^s_{T_R} \, , \tag{76a}$$

with $c^0_{\alpha_R}$ reference (datum) value of the concentration of species. Eqs. (74) take the form

$$\Theta^s_L(c_{L_R}, c_{T_R}) = \frac{\omega^s_L}{1 + \left(c_{L_R} - c^0_{L_R} \right) \, \omega^s_{L_R}} \, , \qquad \Theta^s_T(c_{L_R}, c_{T_R}) = \frac{\omega^s_T}{1 + \left(c_{T_R} - c^0_{T_R} \right) \, \omega^s_{T_R}} . \tag{77a}$$

5.5.2. *Assumptions on* $\boldsymbol{l}^{th}$

Specifications for the thermal velocity gradient are given hereafter with the same structure used in the previous section. Hence, by defining with $f^{th}(T)$, the function which identifies the thermal volumetric Jacobian,

$$J^{th} = f^{th}(T) \, , \tag{78}$$

its time derivative writes as

$$\dot{J}^{th} = \gamma \, \frac{\partial T}{\partial t} \, , \tag{79}$$

where γ denotes the thermal expansion coefficient,

$$\gamma = \frac{\partial f^{th}}{\partial T} . \tag{80}$$

Following the same path of reasoning of Eqs. (74), we find that the ratio $\Theta^{th}(T)$ writes as

$$\Theta^{th}(T) = \frac{\gamma}{J^{th}} = \frac{\gamma}{f^{th}(T)} \, , \tag{81}$$

from which descends the thermal velocity gradient $\boldsymbol{l}^{th}$ as

$$\boldsymbol{l}^{th} = \frac{1}{3} \, \frac{\dot{J}^{th}}{J^{th}} \, \mathbf{1} = \frac{1}{3} \, \Theta^{th} \, \frac{\partial T}{\partial t} \, \mathbf{1}. \tag{82}$$

A classical choice for the function $f^{th}(T)$ is given by the relation

$$f^{th}(T) = 1 + \gamma \, \left(T - T_0 \right) \, , \tag{83}$$

with T_0 the reference (datum) temperature, whence

$$\Theta^{th}(T) = \frac{\gamma}{1 + \gamma \, \left(T - T_0 \right)} . \tag{84}$$

5.5.3. *Definition of* $\mathbf{C}^e$

To make explicit the elastic part of $\mathbf{C}^{cte}$, recall the multiplicative decomposition of $\mathbf{F}^{cte}$ given by Eq. (7), and the definitions of the swelling and thermal deformation gradients, $\mathbf{F}^s$ and $\mathbf{F}^{th}$, shown in Eqs. (65).

The chemo-thermo-elastic deformation gradient can be therefore re-written as

$$\mathbf{F}^{cte} = \mathbf{F}^e \, \mathbf{F}^{th} \, \mathbf{F}^s = \mathbf{F}^e \, \lambda_{th} \, \lambda_s . \tag{85}$$

It follows that, the elastic right Cauchy–Green strain tensor takes the form

$$\mathbf{C}^e = \mathbf{F}^{e^{\mathrm{T}}} \, \mathbf{F}^e = \lambda_s^{-1} \, \lambda_{th}^{-1} \, \mathbf{F}^{cte^{\mathrm{T}}} \, \lambda_s^{-1} \, \lambda_{th}^{-1} \, \mathbf{F}^{cte} = \lambda_s^{-2} \, \lambda_{th}^{-2} \, \mathbf{C}^{cte} = {J^s}^{-\frac{2}{3}} \, {J^{th}}^{-\frac{2}{3}} \, \mathbf{C}^{cte} . \tag{86}$$

6. Constitutive theory

6.1. Helmholtz free energy

The referential Helmholtz free energy density ψ_R is additively decomposed as

$$\psi_R(T, c_{L_R}, c_{T_R}, \mathbf{C}^{cte}, \xi) = \psi_0 + \psi_R^{th}(T, c_{L_R}, c_{T_R}) + \psi_R^{diff}(T, c_{L_R}, c_{T_R}, \mathbf{C}^{cte}, \xi) \\ + \psi_R^{el}(T, c_{L_R}, c_{T_R}, \mathbf{C}^{cte}) + \psi_R^{in}(T, c_{L_R}, c_{T_R}, \xi). \tag{87}$$

Terms in Eq. (87), a detailed analysis of which can be found in Rosakis et al. (2000), have the following meaning. ψ_0 is a datum value; ψ_R^{th} represents the thermal contribution, ψ_R^{diff} the diffusive contributions, ψ_R^{el} the elastic contribution, and ψ_R^{in} is the inelastic counterpart of ψ_R.

Compared to the small strain analysis (Salvadori et al., 2018b), the material description of Eq. (87) entails a dependence of the diffusive contribution upon the strain, as is better reasoned hereinafter.

The thermal contribution $\psi_R^{th}(T, c_{L_R}, c_{T_R})$ is taken of the form

$$\psi_R^{th}(T, c_{L_R}, c_{T_R}) = - \sum_{\alpha=H,L,T} c_{\alpha_R} \, {}^{\eta}\mu_\alpha^0 \left(T - T_0\right) + \frac{1}{2} \, \frac{c_{\upsilon\alpha}^0 \, c_{\alpha_R}}{T_0} \, \left(T - T_0\right)^2 \ , \tag{88}$$

Symbols in Eq. (88) have the following meaning: the subscript H is used to designate the host material, whose concentration, in moles per unit reference volume, is denoted with c_{H_R}; $c_{\upsilon H}^0$, $c_{\upsilon L}^0$, and $c_{\upsilon T}^0$ represent the specific heats of the host material, the diffusive and the trapped species, respectively. The specific heat of each species is taken to be constant and, being (conventionally) energy per mole per degree Kelvin, it multiplies the referential concentration of their respective species, to be converted to energy per unit reference volume.

The transport contribution $\psi_R^{diff}(T, c_{L_R}, c_{T_R}, \mathbf{C}^{cte}, \xi)$ is the referential free energy density of mobile interstitial species that interact with the host material. In the continuum approximation of mixing, it is here described by a regular solution model (Anand, 2012; DeHoff, 2006) which accounts for the entropy of mixing as well as the enthalpic interactions. It has the form

$$\psi_R^{diff}(T, c_{L_R}, c_{T_R}, \mathbf{C}^{cte}, \xi) = \mu_L^0 \, c_{L_R} - T \, \eta_{L_R}^{diff} + \mu_T^0 \, c_{T_R} - T \, \eta_{T_R}^{diff} - T \, \eta_{L_R}^{\chi}. \tag{89}$$

The terms μ_L^0 and μ_T^0 represent reference values of chemical potentials that specify the free energy in the absence of interaction and entropic contributions. Furthermore, by means of μ_L^0 and μ_T^0 it is possible to define the trap energy ΔE_τ, *i.e.*, the negative of the Gibbs free energy change, as

$$\Delta E_\tau = \mu_L^0 - \mu_T^0 = R \, T \, \ln \left[K_{eq} \right] \ , \tag{90}$$

where K_{eq} represents the equilibrium constant of the chemical reaction (11).

The entropy of mixing $\eta_{L_R}^{diff}$ and $\eta_{T_R}^{diff}$ is provided by statistical mechanics, in terms of the density of states $\mathit{\Omega}_\alpha$, by means of the Boltzmann's equation,

$$\eta_{\alpha_R}^{diff} = k_B \, \ln \left[\mathit{\Omega}_{\alpha_R} \right] \ , \tag{91}$$

with k_B the Boltzmann constant. In the case of a two-state system (Shell, 2015),

$$\mathit{\Omega}_{\alpha_R} = \left(\theta_{\alpha_R}^{\theta_{\alpha_R}} \, (1 - \theta_{\alpha_R})^{1 - \theta_{\alpha_R}} \right)^{-N_A \, c_{\alpha_R}^{max}} \ , \tag{92}$$

with N_A Avogadro's number, $c_{\alpha_R}^{max}$ the referential saturation for species α, and θ_{α_R} defined by the ratio

$$\theta_{\alpha_R}(\vec{X}, t) = \frac{c_{\alpha_R}}{c_{\alpha_R}^{max}}. \tag{93}$$

We here assume that, $c_{\alpha_R}^{max}$ being defined on the volume $\mathcal{P}$, it behaves in accordance with the transformation rule (3), and therefore in the same way as the referential concentration defined by Eq. $(16)_1$ (see Fig. 4a). It follows that,

$$c_{\alpha_R}^{max}(\vec{X}, t) = J \, c_\alpha^{max}. \tag{94}$$

Eq. (94) implies that $c_{\alpha_R}^{max}$ is not a constant value, therefore leading to the dependence of the transport contribution $\eta_{\alpha_R}^{diff}$ upon $\mathbf{C}^{cte}$ by means of the Jacobian J.

On the contrary, according to Eqs. $(16)_1$ and (94), the ratio θ_{α_R} (93) is configuration invariant, *i.e.*,

$$\theta_{\alpha_R}(\vec{X}, t) = \theta_\alpha(\vec{x}, t). \tag{95}$$

By entering Eq. (92) into the Boltzmann's equation (91), and recalling the definition of the universal gas constant, $R = k_B N_A$, one finds

$$\eta_{L_R}^{diff} = -R \, c_{L_R}^{max} \, \left(\theta_L \, \ln \left[\theta_L \right] + (1 - \theta_L) \, \ln \left[1 - \theta_L \right] \right). \tag{96}$$

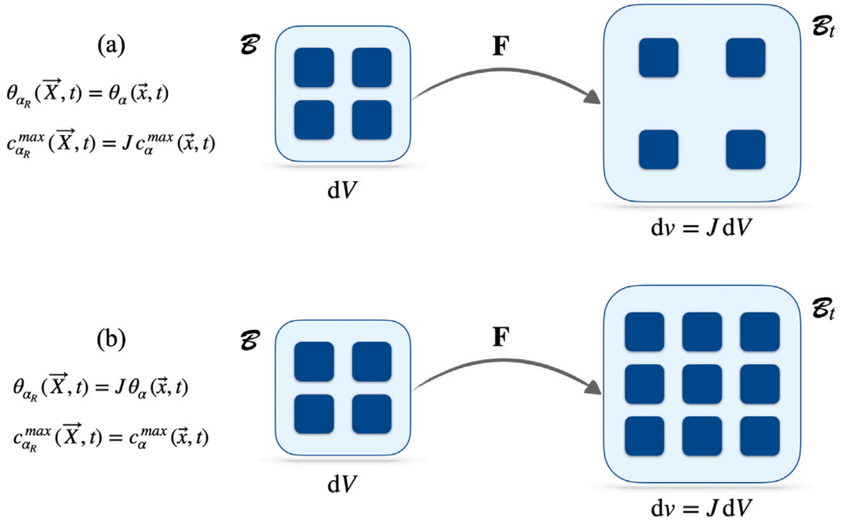

Fig. 4. Depiction of two cases that are paradigms in which (a) the maximum number of moles per unit volume varies with the volumetric Jacobian J, and (b) the maximum number of moles per unit volume is invariant.

The specification for $\eta_{T_R}^{diff}$ has the same form stated by Eq. (96). However, by noting that the saturation limit for trapped species may change in time due to inelastic deformations of the host material, we select a dependence of $c_{T_R}^{max}$ upon ξ. Then

$$\eta_{T_R}^{diff} = -R\,c_{T_R}^{max}(\xi)\ \left(\theta_T(\xi)\ \ln\left[\theta_T(\xi)\right] + (1-\theta_T(\xi))\ \ln\left[1-\theta_T(\xi)\right]\right). \tag{97}$$

Lastly, the excess Gibbs energy writes as

$$-T\,\eta_{L_R}^{\chi} = R\,T\,c_{L_R}^{max}\,\chi\,\theta_L\,\left(1-\theta_L\right) \tag{98}$$

where the Flory interaction parameter χ, also termed the exchange parameter (Shell, 2015), allows us to characterize the energy of interaction between diffusive species and insertion sites of the host material. Eq. (98) endows the free energy density with a nonconvex behavior with respect to c_{L_R} for $\chi > 2$, which in turn may lead to phase segregation (Di Leo et al., 2014; Drozdov, 2014; Bohn et al., 2013). If all interactions between mobile species and host sites are the same, then $\chi = 0$ and there is no enthalpy of mixing, therefore implying an ideal, purely entropic mixing.

Combining Eqs. (96), (97) and (98), the referential diffusive contribution to the Helmholtz free energy re-writes as

$$\begin{aligned}\psi_R^{diff}(T, c_{L_R}, c_{T_R}, \mathbf{C}^{cte}, \xi) = {} & R\,T\,c_{L_R}^{max}\,\chi\,\theta_L\,\left(1-\theta_L\right) \\ & + \sum_{\alpha=L,T} \mu_\alpha^0\,c_{\alpha_R} + R\,T\,c_{\alpha_R}^{max}\,\left(\theta_\alpha\ \ln\left[\theta_\alpha\right] + (1-\theta_\alpha)\ \ln\left[1-\theta_\alpha\right]\right).\end{aligned} \tag{99}$$

The elastic contribution to the free energy can be written in many possible ways, with material parameters changing with concentrations and temperature. In Anand (2012) it is taken in the form

$$\psi_R^{el}(\mathbf{E}^e, c_{L_R}, c_{T_R}) = \frac{1}{2}\,\mathbf{E}^e : \mathbb{C}\mathbf{E}^e\,, \tag{100}$$

with $\mathbf{E}^e = \frac{1}{2}(\mathbf{C}^e - \mathbf{1})$ elastic Green–Lagrange strain tensor and $\mathbb{C}$ a fourth-order tensor given by

$$\mathbb{C} = 2\,G(c_{L_R}, c_{T_R})\,\mathbf{1}^4 + \left(K(c_{L_R}, c_{T_R}) - \frac{2}{3}\,G(c_{L_R}, c_{T_R})\right)\,\mathbf{1}^2 \otimes \mathbf{1}^2\,, \tag{101}$$

where $G(c_{L_R}, c_{T_R})$ and $K(c_{L_R}, c_{T_R})$ represent the bulk and shear modulus, respectively. *Mooney–Rivlin* materials would be written, instead, as

$$\psi_R^{el}(\mathbf{C}^e, c_{L_R}, c_{T_R}) = C_1(c_{L_R}, c_{T_R})\ \left[I_1(\mathbf{C}^e) - 3\right] + C_2(c_{L_R}, c_{T_R})\ \left[I_2(\mathbf{C}^e) - 3\right] \tag{102}$$

with $C_1(c_{L_R}, c_{T_R})$ and $C_2(c_{L_R}, c_{T_R})$ material constants to be empirically determined, and $I_j(\mathbf{C}^e)$ jth invariant of $\mathbf{C}^e$. *Compressible Neo-Hookean* materials would instead be written in the form (Holzapfel, 2001)

$$\psi_R^{el}(\mathbf{C}^e, c_{L_R}, c_{T_R}) = {}^{i}\psi_R^{el}(\mathbf{C}^e, c_{L_R}, c_{T_R}) + {}^{v}\psi_R^{el}(J^e, c_{L_R}, c_{T_R}) \tag{103}$$

with ${}^{i}\psi_R^{el}(\mathbf{C}^e, c_{L_R}, c_{T_R})$ the deviatoric, or isochoric, contribution to the elastic free energy density, usually taken as

$${}^{i}\psi_R^{el}(\mathbf{C}^e, c_{L_R}, c_{T_R}) = \frac{1}{2}\,G(c_{L_R}, c_{T_R})\ \left[{J^e}^{-\frac{2}{3}}\ I_1(\mathbf{C}^e) - 3\right]\,, \tag{104}$$

and ${}^{v}\psi_R^{el}(J^e, c_{L_R}, c_{T_R})$ the volumetric part of the elastic free energy density, which can be assumed to have the forms (see Doll and Schweizerhof (2000))

$$
{}^{v}\psi_R^{el}(J^e, c_{L_R}, c_{T_R}, T) = \frac{1}{2}\, K(c_{L_R}, c_{T_R})\, \ln^2 \left[J^e \right] \,, \tag{105a}
$$

$$
{}^{v}\psi_R^{el}(J^e, c_{L_R}, c_{T_R}, T) = \frac{1}{4}\, K(c_{L_R}, c_{T_R}) \left[\ln^2 \left[J^e \right] + (J^e - 1)^2 \right] \,. \tag{105b}
$$

All these free energies depend upon concentrations intrinsically, *i.e.*, material parameters as the shear and bulk moduli change with the concentration and temperature.

Remark. The ratio θ_{α_R} (93) accounts for the saturation limit $c_{\alpha_R}^{max}$ of the species involved in the chemical reaction (11).

The assumption (94) leads to the configurational invariance of the ratio θ_{α_R}, as specified by Eq. (95). In other words, the number of moles occupying a convecting volume is invariant with time, *i.e.*, it does not change from $\mathcal{B}$ to $\mathcal{B}_t$. The saturation concentration $c_{\alpha_R}^{max}$, on the other hand, is time dependent according to the transformation rule (16). This case is depicted in Fig. 4a.

Conversely, Fig. 4b shows another case in which species can relocate to occupy an eventual volume expansion of the hosting material. The maximum number of moles per unit volume $c_{\alpha_R}^{max}$ is therefore time invariant, *i.e.*, $c_{\alpha_R}^{max}(\vec{X}) = c_{\alpha}^{max}(\vec{x})$. It descends that

$$
\theta_{\alpha_R}(\vec{X}, t) = J\, \theta_\alpha(\vec{x}, t) \,.
$$

6.2. *Contributions to the second Piola–Kirchhoff stress tensor*

It holds that

$$
\mathbf{S}^{cte} = 2\, {J^p}^{-1} \frac{\partial \psi_R^{diff}}{\partial \mathbf{C}^{cte}} + 2\, {J^p}^{-1} \frac{\partial \psi_R^{el}}{\partial \mathbf{C}^{cte}} \,. \tag{106}
$$

To compute the first term, recall that ψ_R^{diff} depends upon $\mathbf{C}^{cte}$ by means of J^{cte}. Therefore, making use of the chain rule, we find

$$
\frac{\partial \psi_R^{diff}}{\partial \mathbf{C}^{cte}} = \frac{\partial \psi_R^{diff}}{\partial J^{cte}} \frac{\partial J^{cte}}{\partial \mathbf{C}^{cte}} = \frac{\partial \psi_R^{diff}}{\partial J^{cte}} \frac{J^{cte}}{2}\, {\mathbf{C}^{cte}}^{-1} \,, \tag{107}
$$

which is a volumetric term induced by the change of the saturation concentration. Furthermore, ψ_R^{el} depends upon $\mathbf{C}^{cte}$ by means of the elastic right Cauchy–Green strain tensor $\mathbf{C}^e$. Indeed, recalling Eq. (86) and the chain rule, one gets

$$
\frac{\partial \psi_R^{el}}{\partial \mathbf{C}^{cte}} = \frac{\partial \psi_R^{el}}{\partial \mathbf{C}^e}\, {J^s}^{-\frac{2}{3}}\, {J^{th}}^{-\frac{2}{3}}\, \mathbf{1}. \tag{108}
$$

Eventually,

$$
\mathbf{S}^{cte} = 2\, {J^p}^{-1} \frac{\partial \psi_R^{diff}}{\partial J^{cte}}\, J^{cte}\, {\mathbf{C}^{cte}}^{-1} + 2\, {J^p}^{-1} \frac{\partial \psi_R^{el}}{\partial \mathbf{C}^e}\, {J^s}^{-\frac{2}{3}}\, {J^{th}}^{-\frac{2}{3}} \,, \tag{109}
$$

Recalling Eqs. (96), (97), (98) and (99), we find

$$
J^{cte} \frac{\partial \psi_R^{diff}}{\partial J^{cte}} = -T\, \eta_{L_R}^{diff} - T\, \eta_{T_R}^{diff} - T\, \eta_{L_R}^{\chi} \,, \tag{110}
$$

where $-T\, \eta_{L_R}^{\chi}$ describes an enthalpic contribution of interactions, whereas the two terms $-T\, \eta_{L_R}^{diff}$ and $-T\, \eta_{T_R}^{diff}$ represent an entropic contribution to the stress.

In conclusion, combining Eqs. (108) and (110), we find that the chemo-thermo-elastic second Piola–Kirchhoff stress tensor writes as

$$
\mathbf{S}^{cte} = -T\, {J^p}^{-1} \left(\eta_{L_R}^{diff} + \eta_{T_R}^{diff} + \eta_{L_R}^{\chi} \right) {\mathbf{C}^{cte}}^{-1} + 2\, {J^p}^{-1} \frac{\partial \psi_R^{el}}{\partial \mathbf{C}^e}\, {J^s}^{-\frac{2}{3}}\, {J^{th}}^{-\frac{2}{3}} . \tag{111}
$$

6.3. *Chemical potential*

Recalling Eqs. (59c), (59d) and (87), one finds that the chemical potential of species α can be constitutively defined via the relation

$$
\mu_\alpha = \frac{\partial \psi_R^{diff}}{\partial c_{\alpha_R}} + \frac{\partial \psi_R^{th}}{\partial c_{\alpha_R}} + \frac{\partial \psi_R^{el}}{\partial c_{\alpha_R}} + \frac{\partial \psi_R^{in}}{\partial c_{\alpha_R}} \tag{112}
$$

whence, according to Eqs. (88) and (99), for $\alpha = L, T$, it holds

$$
\mu_L = \mu_L^0 + R\,T\, \chi \left(1 - 2\, \theta_L \right) + R\,T\, \ln \left[\frac{\theta_L}{1 - \theta_L} \right] - {}^{\eta}\mu_L^0 \left(T - T_0 \right) - \frac{1}{2}\, \frac{c_{v\,L}^{\,0}}{T_0} \left(T - T_0 \right)^2 + \frac{\partial \psi_R^{el}}{\partial c_{L_R}} + \frac{\partial \psi_R^{in}}{\partial c_{L_R}} \,, \tag{113a}
$$

$$\mu_T = \mu_T^0 + R\,T\,\ln\left[\frac{\theta_T}{1-\theta_T}\right] - {}^{\eta}\mu_T^0\,(T-T_0) - \frac{1}{2}\,\frac{c_{vT}^0}{T_0}\,(T-T_0)^2 + \frac{\partial\psi_R^{el}}{\partial c_{T_R}} + \frac{\partial\psi_R^{in}}{\partial c_{T_R}}. \tag{113b}$$

In view of Eqs. (62a) and (113), the change in specific entropy provided by a unit supply of moles of species L and T writes as

$$^{\eta}\mu_L = -\frac{\partial^2\psi_R}{\partial c_{L_R}\partial T} = -\frac{\partial\mu_L}{\partial T} = -R\,\mathbb{\chi}\,(1-2\theta_L) - R\,\ln\left[\frac{\theta_L}{1-\theta_L}\right] + {}^{\eta}\mu_L^0 + \frac{c_{vL}^0}{T_0}\,(T-T_0) - \frac{\partial^2\psi_R^{el}}{\partial T\partial c_{L_R}} - \frac{\partial^2\psi_R^{in}}{\partial T\partial c_{L_R}}, \tag{114a}$$

and

$$^{\eta}\mu_T = -\frac{\partial^2\psi_R}{\partial c_{T_R}\partial T} = -\frac{\partial\mu_T}{\partial T} = -R\,\ln\left[\frac{\theta_T}{1-\theta_T}\right] + {}^{\eta}\mu_T^0 + \frac{c_{vT}^0}{T_0}\,(T-T_0) - \frac{\partial^2\psi_R^{el}}{\partial T\partial c_{T_R}} - \frac{\partial^2\psi_R^{in}}{\partial T\partial c_{T_R}}, \tag{114b}$$

respectively.

6.4. *Heat and mass fluxes*

The thermodynamic restriction (61b) may be satisfied in many possible ways. A classical strategy is to model the flux of interstitial species $\vec{h}_{L_R}$ by Fick's law, and the new heat flux $\vec{\mathbb{q}}_R$ via Fourier's law, by means of positive definite mobility and heat conductivity tensors, $\mathbf{M}_{L_R}$ and $\mathbb{K}$, respectively,

$$\vec{h}_{L_R} = -\mathbf{M}_{L_R}(c_{L_R})\,\mathrm{Grad}\left[\,\mu_L\,\right], \qquad \vec{\mathbb{q}}_R = -\mathbb{K}\,\mathrm{Grad}\,[\,T\,]. \tag{115}$$

As done in Salvadori et al. (2018b), we relate the ordinary heat flux $\vec{q}_R$ to the temperature gradient $\mathrm{Grad}\,[\,T\,]$ via Fourier's law, and the mass flux to the remaining gradients, in view of Eq. (64) and in a consistent way with the thermodynamic restriction (61b). Therefore

$$\vec{h}_{L_R} = -\mathbf{M}_{L_R}(c_{L_R})\,\left(\mathrm{Grad}\left[\,\mu_L\,\right] + {}^{\eta}\mu_L\,\mathrm{Grad}\,[\,T\,]\right), \tag{116a}$$

$$\vec{q}_R = -\mathbb{K}\,\mathrm{Grad}\,[\,T\,]. \tag{116b}$$

To account for saturation and to satisfy the physical requirement that both the pure and the saturated phases, $c_{L_R} = 0$ and $c_{L_R} = c_{L_R}^{max}$, lead to vanishing mobility, the mobility tensor $\mathbf{M}_{L_R}(c_{L_R})$ is chosen in the following isotropic nonlinear form (Anand, 2012)

$$\mathbf{M}_{L_R}(c_{L_R}) = \mathbb{u}_L\,c_{L_R}^{max}\,\theta_L\,\left(1-\theta_L\right)\mathbf{1}, \tag{117}$$

with $\mathbb{u}_L > 0$ the mobility of interstitial chemical species, and $c_{L_R}^{max}$ and θ_L defined by Eqs. (94) and (93), respectively.

To formulate Fick's law (116a), recall how the vector $\mathrm{Grad}\left[\,\mu_L\,\right] + {}^{\eta}\mu_L\,\mathrm{Grad}\,[\,T\,]$ has been defined in Eq. (64). Then

$$\begin{aligned}\vec{h}_{L_R} = -\mathbf{M}_{L_R}(c_{L_R})\Bigg(&\frac{\partial^2\psi_R}{\partial c_{L_R}^2}\,\mathrm{Grad}\left[\,c_{L_R}\,\right] + \frac{\partial^2\psi_R}{\partial c_{L_R}\partial c_{T_R}}\,\mathrm{Grad}\left[\,c_{T_R}\,\right]\,\frac{\partial^2\psi_R}{\partial c_{L_R}\partial\mathbf{C}^{cte}} : \mathrm{Grad}\left[\,\mathbf{C}^{cte}\,\right]\\ &+ \frac{\partial^2\psi_R}{\partial c_{L_R}\partial\xi} : \mathrm{Grad}\,[\,\xi\,]\Bigg).\end{aligned} \tag{118}$$

The first term in brackets of Eq. (118) writes as

$$\frac{\partial^2\psi_R}{\partial c_{L_R}^2}\mathrm{Grad}\left[\,c_{L_R}\,\right] = R\,T\,\frac{1}{c_{L_R}^{max}}\left(\frac{1}{\theta_L(1-\theta_L)} - 2\,\mathbb{\chi}\right)\mathrm{Grad}\left[\,c_{L_R}\,\right] + \frac{\partial^2\psi_R^{el}}{\partial c_{L_R}^2}\mathrm{Grad}\left[\,c_{L_R}\,\right] + \frac{\partial^2\psi_R^{in}}{\partial c_{L_R}^2}\mathrm{Grad}\left[\,c_{L_R}\,\right], \tag{119}$$

whereas the last three terms in brackets of Eq. (118) take the form

$$\frac{\partial^2\psi_R}{\partial c_{L_R}\partial c_{T_R}}\,\mathrm{Grad}\left[\,c_{T_R}\,\right] = \frac{\partial^2\psi_R^{el}}{\partial c_{L_R}\partial c_{T_R}}\,\mathrm{Grad}\left[\,c_{T_R}\,\right] + \frac{\partial^2\psi_R^{in}}{\partial c_{L_R}\partial c_{T_R}}\,\mathrm{Grad}\left[\,c_{T_R}\,\right], \tag{120a}$$

$$\frac{\partial^2\psi_R}{\partial c_{L_R}\partial\mathbf{C}^{cte}} : \mathrm{Grad}\left[\,\mathbf{C}^{cte}\,\right] = \frac{\partial^2\psi_R^{el}}{\partial c_{L_R}\partial\mathbf{C}^{cte}} : \mathrm{Grad}\left[\,\mathbf{C}^{cte}\,\right], \tag{120b}$$

$$\frac{\partial^2\psi_R}{\partial c_{L_R}\partial\xi} : \mathrm{Grad}\,[\,\xi\,] = \frac{\partial^2\psi_R^{in}}{\partial c_{L_R}\partial\xi} : \mathrm{Grad}\,[\,\xi\,]. \tag{120c}$$

Taking advantage of the definition of the mobility tensor $\mathbf{M}_{L_R}(c_{L_R})$ given by Eq. (117), and by defining the interstitial diffusivity according to Einstein's equation, we deduce that

$$\mathbb{D}_L = \mathbb{u}_L\,R\,T,$$

and simple algebra allows us to re-write the Fick's law (116a) as

$$
\begin{aligned}
\vec{h}_{L_R} = & -\mathbb{D}_L \left[1 - 2\,\chi\theta_L(1-\theta_L)\right] \text{Grad}\left[c_{L_R}\right] \\
& - \mathbf{M}_{L_R} \left(\frac{\partial^2 \psi_R^{el}}{\partial c_{L_R}^2} \text{Grad}\left[c_{L_R}\right] + \frac{\partial^2 \psi_R^{el}}{\partial c_{L_R} \partial c_{T_R}} \text{Grad}\left[c_{T_R}\right] + \frac{\partial^2 \psi_R^{el}}{\partial c_{L_R} \partial \mathbf{C}^{cte}} : \text{Grad}\left[\mathbf{C}^{cte}\right] \right) \\
& - \mathbf{M}_{L_R} \left(\frac{\partial^2 \psi_R^{in}}{\partial c_{L_R}^2} \text{Grad}\left[c_{L_R}\right] + \frac{\partial^2 \psi_R^{in}}{\partial c_{L_R} \partial c_{T_R}} \text{Grad}\left[c_{T_R}\right] + \frac{\partial^2 \psi_R^{in}}{\partial c_{L_R} \partial \xi} : \text{Grad}\left[\xi\right] \right).
\end{aligned}
\tag{121}
$$

7. Chemical kinetics

For an ideal system, in which the solvent does not take part in reactions, the kinetics of reaction (11) is well modeled via the following law of mass action (De Groot and Mazur, 1984)

$$
w_R^{(11)}(\vec{X},t) = k_{T_R} \frac{\theta_L}{1-\theta_L} - k_{L_R} \frac{\theta_T}{1-\theta_T}.
\tag{122}
$$

In agreement with the transformation $(16)_2$ of $w_R^{(11)}$ defined by Eq. (3), the rate factors for both the forward and reverse reaction, k_{T_R} and k_{L_R}, transform according to

$$
k_{\alpha_R}(\vec{X},t) = J\, k_\alpha \,,
\tag{123}
$$

therefore both k_{T_R} and k_{L_R} are not constant values, rather they evolve with the deformation of the body by means of J.

Furthermore, following what is proposed in Salvadori et al. (2018b), the variation in time of $k_{\alpha_R}(\vec{X},t)$ is related to the stress and to the concentration of species via elastic parameters. Consequently, the referential rate factor which describes the reverse reaction is taken as

$$
k_{L_R} = \tilde{k}_{L_R} \exp\left(\frac{1}{RT} \frac{\partial \psi_R^{el}}{\partial c_{T_R}} \right) \exp\left(\frac{1}{RT} \frac{\partial \psi_R^{in}}{\partial c_{T_R}} \right) \exp\left(-\frac{{}^{\eta}\mu_T^0\,(T-T_0)}{RT} \right) \exp\left(-\frac{c_{\upsilon T}^0 (T-T_0)^2}{2\,RT\,T_0} \right) ,
\tag{124a}
$$

whereas the referential factor providing the description of the forward reaction has the form

$$
\begin{aligned}
k_{T_R} = & \tilde{k}_{T_R} \exp\left(\frac{1}{RT} \frac{\partial \psi_R^{el}}{\partial c_{L_R}} \right) \exp\left(\frac{1}{RT} \frac{\partial \psi_R^{in}}{\partial c_{L_R}} \right) \exp\left(-\frac{{}^{\eta}\mu_L^0\,(T-T_0)}{RT} \right) \exp\left(-\frac{c_{\upsilon L}^0 (T-T_0)^2}{2\,RT\,T_0} \right) \\
& \exp\left(\chi(1-2\,\theta_L) \right).
\end{aligned}
\tag{124b}
$$

Therefore, the factors k_{L_R} and k_{T_R}, with respect to the small strain analysis prescriptions (Salvadori et al., 2018b), are no longer constants, given that they follow the same transformation rule for $k_{\alpha_R}(\vec{X},t)$ shown in Eq. (123) and defined by Eq. (3). This new formulation is consistent with the usual mass action law described by the *van't Hoff* relation (Shell, 2015), which is recovered when elastic, swelling, and interaction contributions vanish.

The condition of null affinity, $A^{(11)} = 0$, can be solved for the Gibbs free energy change, $\mu_L^0 - \mu_T^0$, in order to obtain the equilibrium constant K_{eq} of the chemical reaction (11). According to the definition (40) of the affinity $A^{(11)}$, and re-writing Eq. (90) to obtain K_{eq}, we find

$$
K_{eq} = \exp\left(\frac{\Delta E_\tau}{RT} \right) = \exp\left(\frac{\mu_L^0 - \mu_T^0}{RT} \right) ,
\tag{125}
$$

The terms μ_L^0 and μ_T^0 can be derived by means of the constitutive definition of the chemical potentials (113a) and (113b), respectively. Accordingly, the term $\mu_L^0 - \mu_T^0$ of Eq. (125) writes at equilibrium as

$$
\begin{aligned}
\mu_L^0 - \mu_T^0 = & -RT\,\chi\left(1 - 2\,\theta_L^{eq}\right) + RT \left(\ln\left[\frac{\theta_T^{eq}}{1-\theta_T^{eq}}\right] - \ln\left[\frac{\theta_L^{eq}}{1-\theta_L^{eq}}\right] \right) + \left({}^{\eta}\mu_L^0 - {}^{\eta}\mu_T^0\right)\left(T^{eq} - T_0\right) \\
& + \frac{1}{2}\left(\frac{c_{\upsilon L}^0 - c_{\upsilon T}^0}{T_0} \right)\left(T^{eq} - T_0\right)^2 + \left(\frac{\partial \psi_R^{el}}{\partial c_{T_R}} - \frac{\partial \psi_R^{el}}{\partial c_{L_R}} \right) + \left(\frac{\partial \psi_R^{in}}{\partial c_{T_R}} - \frac{\partial \psi_R^{in}}{\partial c_{L_R}} \right) ,
\end{aligned}
$$

whence, the equilibrium constant K_{eq} of the chemical reaction (11) writes as

$$
\begin{aligned}
K_{eq} = & \frac{\theta_T^{eq}}{1-\theta_T^{eq}} \, \frac{1-\theta_L^{eq}}{\theta_L^{eq}} \, \exp\left[-\chi\left(1-2\,\theta_L^{eq}\right)\right] \\
& \exp\left[\frac{{}^{\eta}\mu_L^0 - {}^{\eta}\mu_T^0}{RT} \left(T^{eq} - T_0\right) \right] \exp\left[\frac{1}{2} \frac{c_{\upsilon L}^0 - c_{\upsilon T}^0}{RT\,T_0} \left(T^{eq} - T_0\right)^2 \right] \\
& \exp\left[\frac{1}{RT} \left(\frac{\partial \psi_R^{el}}{\partial c_{T_R}} - \frac{\partial \psi_R^{el}}{\partial c_{L_R}} \right) \right]^{eq} \exp\left[\frac{1}{RT} \left(\frac{\partial \psi_R^{in}}{\partial c_{T_R}} - \frac{\partial \psi_R^{in}}{\partial c_{L_R}} \right) \right]^{eq} .
\end{aligned}
\tag{126}
$$

An alternative way to derive K_{eq} is by imposing $w_R^{(11)} = 0$ in Eq. (122). In this instance, the equilibrium constant of reaction (11) writes as

$$K_{eq} = \frac{\tilde{k}_{T_R}}{\tilde{k}_{L_R}}$$

and Eq. (126) is recovered by taking advantage of Eqs. (124) to express $\tilde{k}_T$ and $\tilde{k}_L$.

The thermodynamic restriction

$$w_R^{(11)} \, A^{(11)} \leq 0$$

is satisfied by means of Eqs. (124). Furthermore, a classical way to enforce thermodynamic restrictions for the chemical reaction (11) is to select a positive phenomenological coefficient, usually termed $L^{(11)}$, which linearly relates the affinity, $A^{(11)}$, to the reaction rate, $w_R^{(11)}$, via the relation

$$w_R^{(11)} = -L^{(11)} \, A^{(11)} \, .$$

The proof of these two last statements is not influenced by finite strains and can be found in Salvadori et al. (2018b).

8. Governing equations

The governing equations are obtained by incorporating the constitutive prescriptions of the chemo-thermo-elastic second Piola–Kirchhoff stress tensor $\mathbf{S}^{cte}$ (111), the referential heat and mass flux vectors, $\vec{q}_R$ and $\vec{h}_{L_R}$, given by Eqs. (116b) and (121), respectively, and the mass action law (122) with specifications (124), into the balance Eqs. (15), (21), and (127d). Governing equations are written in term of the state variables c_{L_R}, c_{T_R}, $\vec{u}$, and T. They read

$$\frac{\partial c_{L_R}}{\partial t} + \mathrm{Div}\left[\vec{h}_{L_R}(c_{L_R}, c_{T_R}, T, \mathbf{C}^{cte}, \xi) \right] + w_R^{(11)}(c_{L_R}, c_{T_R}, T, \mathbf{C}^{cte}, \xi) = s_{L_R} \, , \tag{127a}$$

$$\frac{\partial c_{T_R}}{\partial t} - w_R^{(11)}(c_{L_R}, c_{T_R}, T, \mathbf{C}^{cte}, \xi) = s_{T_R} . \tag{127b}$$

$$\mathrm{Div}\left[\mathbf{P}\,(\mathbf{S}^{cte}, \mathbf{C}^{cte}, c_{L_R}, c_{T_R}, T) \right] + \vec{b}_R^0 = \vec{0} \, , \tag{127c}$$

$$\begin{aligned} & -T \, \frac{\partial^2 \psi_R}{\partial T^2} \, \frac{\partial T}{\partial t} - \mathrm{Div}\left[\mathbb{K} \, \mathrm{Grad}\,[\, T \,] \right] = T \, \frac{\partial^2 \psi_R}{\partial T \partial \mathbf{C}^{cte}} \; : \; \frac{\partial \mathbf{C}^{cte}}{\partial t} + J^p \, \mathbf{M}^{cte} \; : \; \boldsymbol{l}^p + s_{q\,R} + \\ & + \left(\chi + T \frac{\partial^2 \psi_R}{\partial T \partial \xi} \right) \; : \; \frac{\partial \xi}{\partial t} + \mathbf{M}_{L_R}(c_{L_R}) \left(\mathrm{Grad}\left[\, \mu_L \, \right] + {}^{\eta}\mu_L \mathrm{Grad}\,[\, T \,] \right) \cdot \mathrm{Grad}\left[{}^{u}\mu_L \right] + \left({}^{u}\mu_L - {}^{u}\mu_T \right) w_R^{(11)} . \end{aligned} \tag{127d}$$

Details of the derivation of Eq. (127d) have been collected in Appendix A.2.

The boundary conditions

$$\vec{h}_{L_R} \cdot \vec{n}_R = \overline{h}_R \qquad \vec{X} \in \partial^N V \, , \tag{128a}$$

$$\vec{q}_R \cdot \vec{n}_R = \overline{q}_R \qquad \vec{X} \in \partial^N V \, , \tag{128b}$$

$$\mathbf{P} \, \vec{n}_R = \overline{\vec{t}_R} \qquad \vec{X} \in \partial^N V \, , \tag{128c}$$

are imposed along Neumann boundaries $\partial^N V$. To ensure solvability of the problem, Dirichlet boundary conditions have to be enforced along the complementary boundary $\partial^D V$, hence

$$T = \overline{T} \qquad \vec{X} \in \partial^D V \, , \tag{129a}$$

$$\vec{u} = \overline{\vec{u}} \qquad \vec{X} \in \partial^D V . \tag{129b}$$

Initial conditions are usually imposed for the concentration of interstitial species, $c_{L_R}(\vec{X}, t = 0)$, as well as of trapped species $c_{T_R}(\vec{X}, t = 0)$ and temperature, $T(\vec{X}, t = 0)$. To comply with equilibrium thermodynamics these conditions are chosen to be uniform in the material and to ensure equilibrium with external species. Balance of momentum, together with boundary conditions, provide the necessary and sufficient equations and conditions to solve for $\vec{u}$ at $t = 0$.

9. Numerical simulations

Focused ion beam implantation (Li-FIB) has been introduced as a new approach to probe lithiation mechanisms in the active particles of Li-ion batteries (Takeuchi et al., 2016). In this process, a FIB with small spot size is directed at a particle in vacuum and scanned across the sample. Experimental evidence (see Figures 1 and 2 in Takeuchi et al. (2016)) show a lithiated zone, associated with a band of contrast starting from the insertion area and expanding into the particle, causing a volume change of a factor of

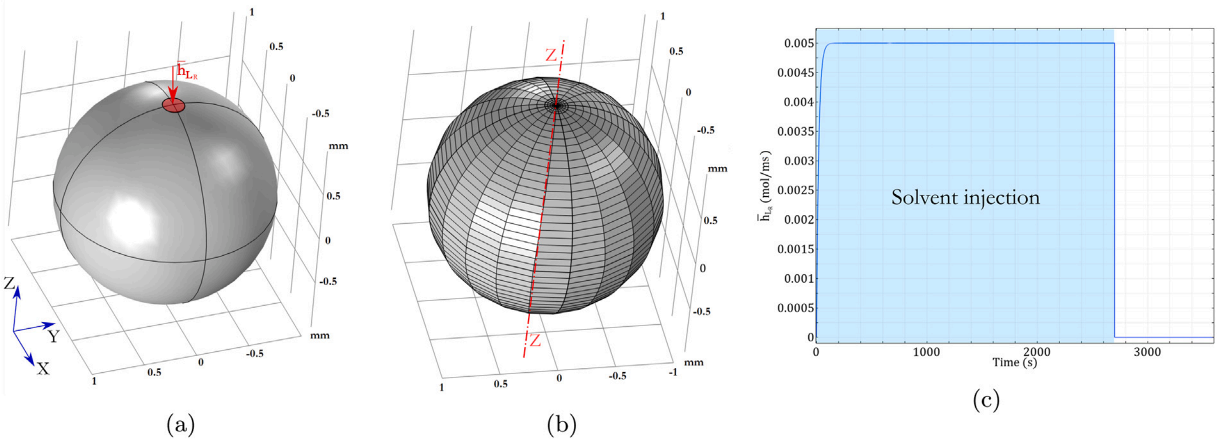

(a) (b) (c)

Fig. 5. (a) Schematic representation of the geometry selected for the three-dimensional example. In red the surface where species L insertion takes place has been highlighted. (b) An unstructured grid depicts the FE discretization adopts in COMSOL Multiphysics. (c) Plot of the imposed mass flux of species, $\vec{h}_{L_R} \cdot \vec{n}_R = \overline{h}_R$, as a function of time.

$\simeq$ 2.3 (Takeuchi et al., 2016). Such a large volume expansion is not compatible with the small strain theory developed in Part 1 (Salvadori et al., 2018b). Exploiting therefore the theory developed in this paper, we simulate the Li-FIB approach on a host spherical particle and show how mobile species enter, diffuse, and immobilize because of chemical trapping. Simulations illustrate the methodology in terms of proof of concept, without direct reference to real data of lithiation.

For the sake of simplicity of notation, we keep the symbols L and T to denote the mobile and trapped Li-ion species. We select a host spherical particle of radius $r = 1$ mm, taken as the reference configuration $\mathcal{B}$. An inward mass flux, $\vec{h}_{L_R}$, enters the body perpendicularly to the sphere

$$\vec{h}_{L_R}(\vec{X}) \cdot \vec{n}_R(\vec{X}) = \overline{h}_R \, , \qquad \vec{X} \in \partial^N V \, , \tag{130}$$

at the apical sub-area $\partial^N V$ of its surface, as shown in Fig. 5a. The projection of $\partial^N V$ onto the equator plane is a circle of radius $r_{ins} = 0.1$ mm. After a transient regime in which the uniform mass flux increases, $\overline{h}_R$ is held constant in time at 0.005 mol/m^{2}s, prior to being removed at time $t = 2700$ s, as depicted in Fig. 5c. For the sake of simplicity, we assume thermal equilibrium at a constant temperature of 25 °C. The diffusivity of the mobile species, $\text{Đ}_L = 1.00 \times 10^{-9}$ m^2/s, is assumed to be concentration-independent.

All material parameters used in the simulations are listed in Table 1.

For the sake of simplicity, we assume an irreversible trapping process, described in abstract form by the chemical reaction (11), with a permanent modification of the host material. The law of mass action (122), simplifies as

$$w_R^{(11)}(\vec{X}, t) = \tilde{k}_{T_R} \exp\left[\, \chi (1 - 2\,\theta_L) \right] \, \frac{\theta_L}{1 - \theta_L} \, , \tag{131}$$

with $\tilde{k}_{T_R} = 1$ mol/m^{3}s. Moreover, we assume $f_L^s(c_{L_R}) = 1$ and

$$J^s = 1 + \left(c_{T_R} - c_{T_R}^0 \right) \omega_{T_R}^s \, , \tag{132}$$

i.e., only the alligated species induce a volume change in the host particle.

The elastic Saint Venant–Kirchhoff free energy (100) models the mechanical response of the particle, with elastic parameters $G = 79.3$ GPa and $K = 206.8$ GPa taken as independent of the concentration of species. The chemo-thermo-elastic second Piola–Kirchhoff stress tensor coincides with the total stress in the material, $\mathbf{S} = \mathbf{S}^{cte}$, and Eq. (111) re-writes as

$$\mathbf{S} = R\,T\,\xi\,\mathbf{C}^{-1} + \mathbb{C}\,\mathbf{E}^e \, {J^s}^{-\frac{2}{3}} \, , \tag{133}$$

with $\mathbb{C} = 2\,G\,\mathbf{1}^4 + \lambda\,\mathbf{1}^2 \otimes \mathbf{1}^2$, $\mathbf{C} = {J^s}^{\frac{2}{3}}\,\mathbf{C}^e$, and

$$\xi = c_{L_R}^{max} \left\{ \chi\theta_L \left(1 - \theta_L\right) + \theta_L \ln\left[\theta_L\right] + (1 - \theta_L) \ln\left[1 - \theta_L\right] \right\} + c_{T_R}^{max} \left\{ \theta_T \ln\left[\theta_T\right] + (1 - \theta_T) \ln\left[1 - \theta_T\right] \right\} .$$

Denote with Đ_L^* a diffusion-like parameter, defined as

$$\text{Đ}_L^* = \text{Đ}_L \left[1 - 2\,\chi\theta_L (1 - \theta_L) \right] . \tag{134}$$

The mass flux (121) reduces to

$$\vec{h}_{L_R} = -\text{Đ}_L^* \ \mathrm{Grad}\left[c_{L_R} \right] . \tag{135}$$

Table 1
Model parameters used for numerical simulations.

Input parameters			
Parameters	Value	Unit of measure	Description
T	298.15	K	Temperature
r	1.00	mm	Radius of the sphere
r_{ins}	0.10	mm	Radius of the insertion area of species L
$\mathbb{D}_{\mathrm{L}}$	$1.00 \cdot 10^{-9}$	m^2/s	Diffusion coefficient for the species L
$\tilde{k}_{T_R}$	1.00	$\mathrm{mol/m^3\ s}$	T generation reaction rate constant, Eq. (122)
$\tilde{k}_{L_R}$	0	$\mathrm{mol/m^3\ s}$	L recombination reaction rate constant, Eq. (122)
G	$79.3 \cdot 10^3$	MPa	Shear modulus
K	$206.8 \cdot 10^3$	MPa	Bulk modulus
$\omega^s_{L_R}$	0	$\mathrm{m^3/mol}$	Swelling expansion coefficient of species L
$\omega^s_{T_R}$	$1.0 \cdot 10^{-6}$	$\mathrm{m^3/mol}$	Swelling expansion coefficient of species T
χ	0*	–	Flory–Huggins interaction parameter
$c^{max}_{L_R}$	$1.0 \cdot 10^4$	$\mathrm{mol/m^3}$	Saturation limit concentration for species L
$c^{max}_{T_R}$	$1.0 \cdot 10^4$	$\mathrm{mol/m^3}$	Saturation limit concentration for species T

The governing Eq. (127) take the form

$$\frac{\partial c_{L_R}}{\partial t} + \mathrm{Div}\left[\vec{h}_{L_R}(c_{L_R}, c_{T_R}, \mathbf{C}^{cte})\right] = -w_R^{(11)}(c_{L_R}, c_{T_R}, \mathbf{C}^{cte}) \,, \tag{136a}$$

$$\frac{\partial c_{T_R}}{\partial t} = w_R^{(11)}(c_{L_R}, c_{T_R}, \mathbf{C}^{cte}) \,, \tag{136b}$$

$$\mathrm{Div}\left[\mathbf{F}\,\mathbf{S}(c_{L_R}, c_{T_R}, \mathbf{C}^{cte})\right] + \vec{b}_R^0 = \vec{0}. \tag{136c}$$

The partial differential Eq. (136) are solved using the Finite Element Software COMSOL Multiphysics by means of the "PDE Interface", which provides an environment for specifying a model in terms of equations in strong form. The time-dependent solver uses the implicit time-stepping methods BDF (Backward Differentiation Formula). A time interval of 3600 s has been considered with a free timestepping. The solver takes timesteps as large as possible ($\Delta t = 1$ s), but it reduces the timestep size when necessary if the solution starts to vary rapidly in time. The Neumann boundary condition (130) is imposed together with

$$\mathbf{P}\,\vec{n}_R = \vec{0} \,, \qquad \vec{X} \in \partial^N V. \tag{137}$$

Surface traction forces are set to zero to allow free expansion and contraction of the particle. The initial conditions on the concentration of species are imposed as

$$c_{L_R}(\vec{X}, t = 0) = 10 \ \mathrm{mol/m^3} \,, \quad c_{T_R}(\vec{X}, t = 0) = 10 \ \mathrm{mol/m^3} \,. \tag{138}$$

9.1. Concentration and displacement fields

The inward flow $\overline{h}_R$ of species L into the particle occurs in a narrow FIB spot size for the first 2700 s. In that time span, the mobile species is transported within the particle at a low pace compared to the FIB influx. Therefore, L species accumulates at the apical side, where c_{L_R} reaches a maximum value of 521.8 mol m^{-3}. Concentrations c_{L_R} and c_{T_R} at the end of the inward flow are portrayed in Fig. 6a and d, respectively. Arrows in Fig. 6a depict the streamlines of the $\vec{h}_{L_R}$ flux. A portion of species L is immediately alligated into trapped species, T, ruled by the chemical reaction (131), see Fig. 6d.

After the inflow quits, mobile species diffuse through the particle according to Fick's law (135). A reduction in the peak of c_{L_R} at the apical side of the particle takes place, becoming more and more pronounced with time as seen in Fig. 6c. An almost uniform concentration is reached at 3600 s. Fig. 6b depicts the profile of c_{L_R} at time $t = 2760$ s.

Since trapped species cannot be re-converted into mobile species, the concentration c_{T_R} does not decrease in time — see Fig. 6f; rather, it increases slightly, in view of the continuous conversion of species L into T in Eq. (131). A plot of c_{T_R} at time $t = 2760$ s is shown in Fig. 6e.

The concentration fields c_{L_R} and c_{T_R} are displayed in a particle cross-section in Fig. 7. The scenario described above is recovered.

The trapping provides a chemo-mechanical increment in volume, dictated by the coefficient $\omega^s_{T_R}$ in Eq. (132). Fig. 8 manifests the swelling, with c_{T_R} inferred from Fig. 6f.

Fig. 8 plots the norm of the displacement field in the current configuration. The referential spherical configuration, attained at time $t = 0$ s, is shown as a black circle. Three different time steps are considered; at $t = 300$ s, a strictly localized displacement field occurs in the proximity of the insertion area (Fig. 8a). At time $t = 2700$ s the particle has already assumed a drop-like shape, as shown in Fig. 8b. Eventually, at $t = 3600$ s the mobile species uniformly occupy the domain and the maximal expansion of the body is achieved.

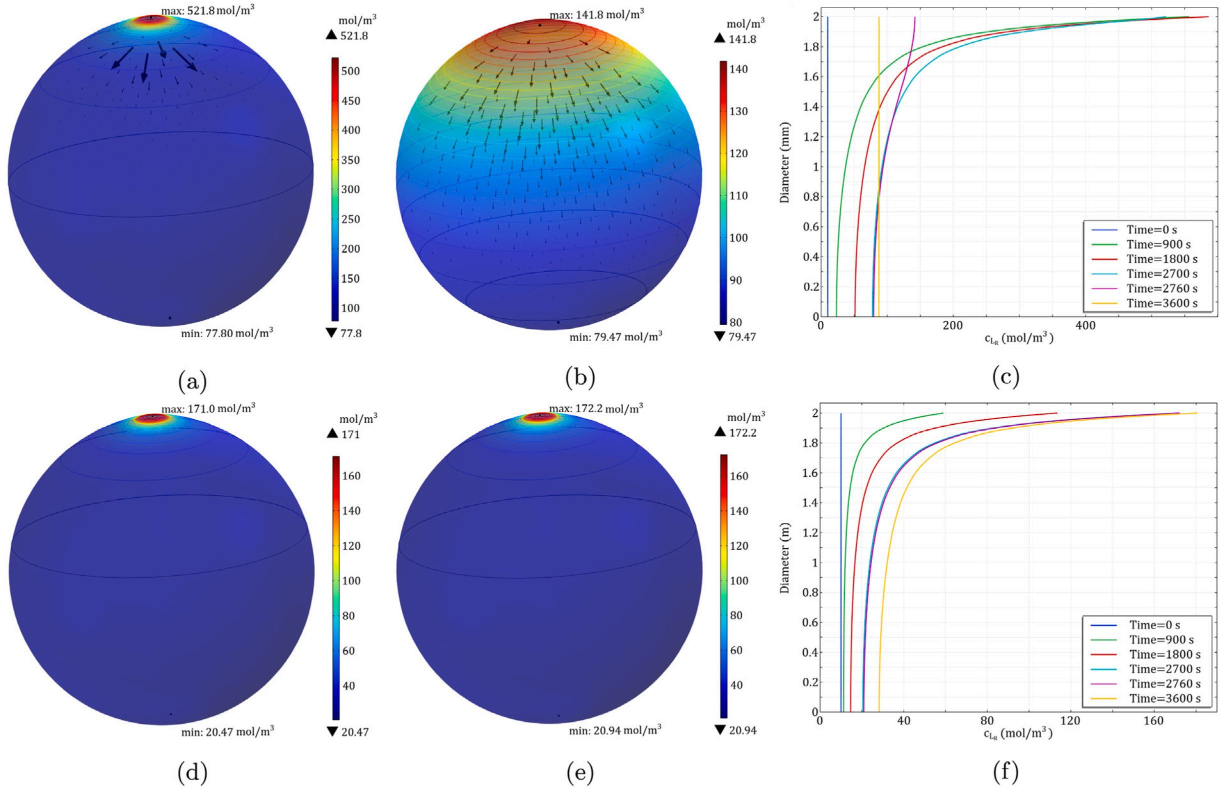

Fig. 6. Contour plots of the concentrations c_{L_R} (a, b) and c_{T_R} (d, e), at time $t = 2700$ s, (a) and (d), on the left, and $t = 2760$ s, (b) and (e), on the right. Concentration of species (c) c_{L_R} and (f) c_{T_R} along the diameter aligned with the symmetry axis Z-Z in Fig. 5b (origin in the bottom of the sphere), at different time steps.

9.2. *Effect of the Flory–Huggins parameter*

Simulations carried out in Section 9.1 have been performed at a vanishing Flory–Huggins parameter, $\chi = 0$. In order to investigate the influence of the Flory–Huggins parameter, we set $\mu^0_L = 0$ and $\mu^0_T = 0$ and re-write the referential entropic Helmholtz free energy as

$$\psi_R^{diff} = R\,T\,c_{L_R}^{max}\,\chi\,\theta_L\,\left(1-\theta_L\right) + \sum_{\alpha=L,T} R\,T\,c_\alpha^{max}\,\left(\theta_\alpha\,\ln\left[\theta_\alpha\right] + (1-\theta_\alpha)\,\ln\left[1-\theta_\alpha\right]\right) \tag{139}$$

from Eq. (99).

The shape of ψ_R^{diff} has been portrayed in Fig. 9a as a function of the normalized concentration of species L and T, and in Fig. 9b–c restricted to $\theta_T = 0$. Fig. 9b shows the evolution of the entropic free energy at increasing values of the Flory–Huggins parameters. For $\chi = 0$, no interactions of mobile species with the host material occur, representing ideal mixing. Positive values of χ account for the energetic interactions between species L and the host material. As a result, the mixing deviates from the ideal scenario. The value of the Flory–Huggins parameter $\chi = 2$ is a threshold for the energy of mixing. At $\chi \leq 2$ there is a single-well chemical free energy, leading to a uniform distribution of mobile species at equilibrium. If $\chi > 2$, the non-convex double-well potential may result in the accumulation of mobile species in localized regions of the body.

Similar conclusions can be reached from assessments of Eq. (135) in regard to the mass flux $\vec{h}_{L_R}$ for different values of the Flory–Huggins parameter χ. Fig. 9c shows that $\mathbb{D}^*_L > 0$ for $\chi < 2$. Accordingly, the species move from higher to lower concentration, as is normal. As the Flory–Huggins parameter increases, energetic interactions act against this behavior and at $\chi = 2$ the diffusivity $\mathbb{D}^*_L$ vanishes. For $\chi > 2$, $\mathbb{D}^*_L$ becomes negative for each value of θ_L that makes the free energy concave (compare Fig. 9b and c) yielding an inversion in the mass flux. The resulting motion of the species assumes a counter-intuitive behavior; diffusion from lower to higher concentration becomes possible and segregation of mobile species can be observed.

The rate of trapping of species L increases with χ. The prominent influence of the Flory–Huggins parameter on the generation of trapped species is clearly seen in Eq. (131). The forward reaction is driven by the exponential term

$$\exp\left(\chi(1-2\,\theta_L)\right)\ ,$$

which greatly affects the trapping of L. In this regard the Flory–Huggins parameter works against the segregation of mobile species, because the consumption of L may not allow c_{L_R} to reach the range in which $\mathbb{D}^*_L$ becomes negative. For this case, no

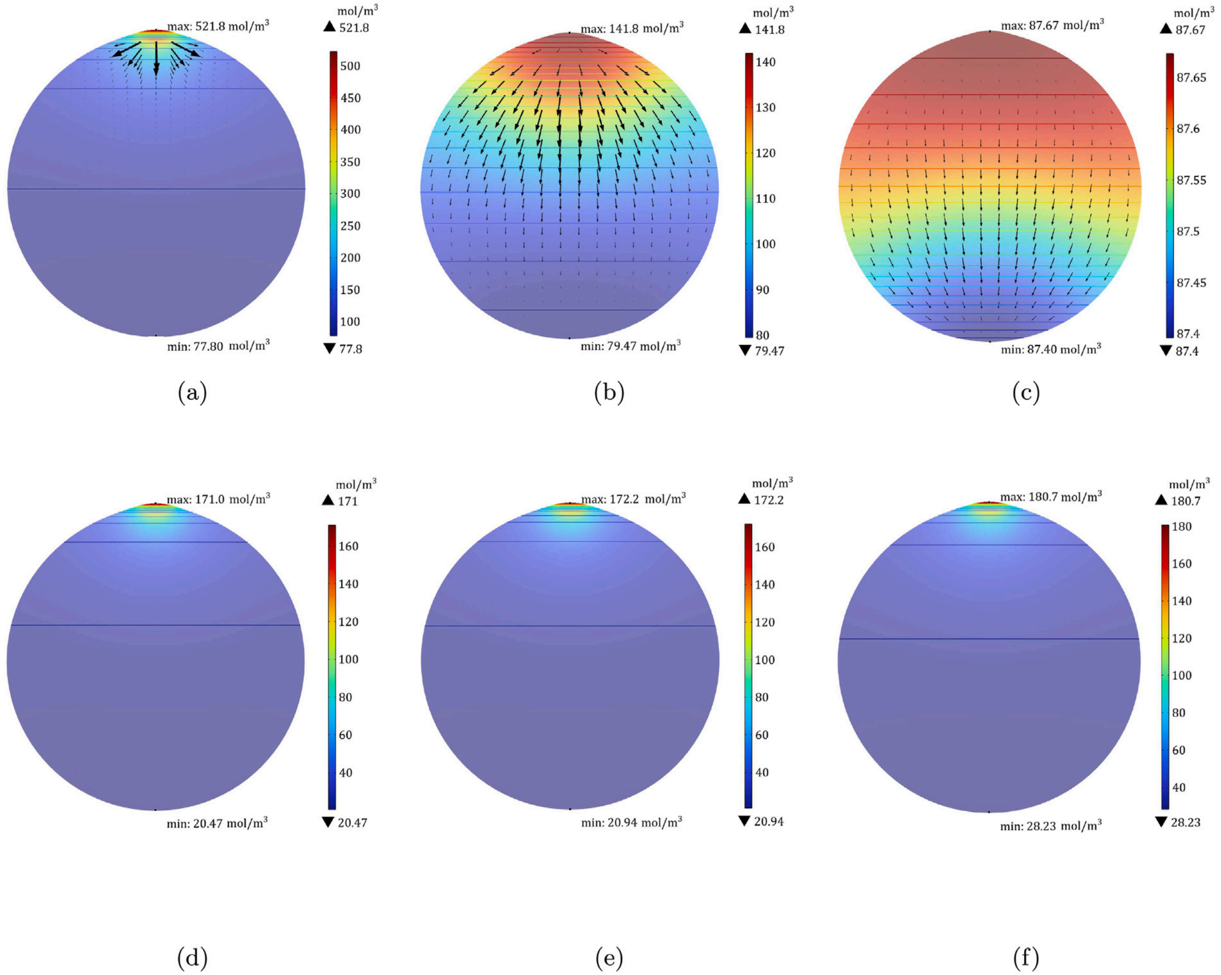

Fig. 7. Density plots of c_{L_R} and c_{T_R} at time (a, d) $t = 2700$ s, (b, e) $t = 2760$ s, and (c, f) $t = 3600$ s, respectively. Black arrows (a, b, c) represent the mass flux, $\vec{h}_{L_R}$.

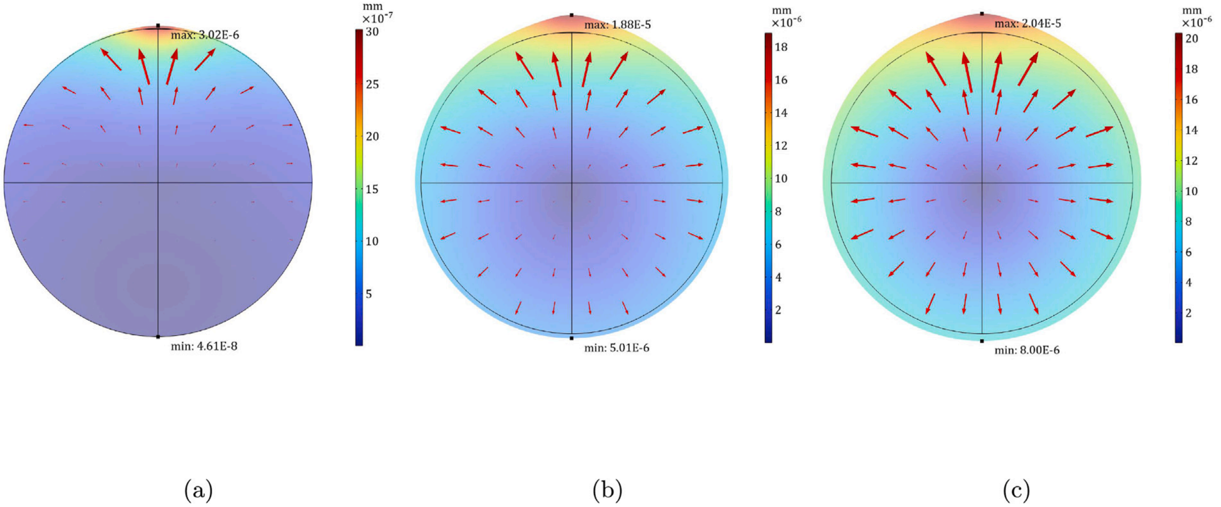

Fig. 8. Plots of the norm of the displacement field $\delta = \| \vec{u} \|$ in a transversal section of the sphere at the time step $t = 300$ s (a), $t = 2700$ s (b), and $t = 3600$ s (c).

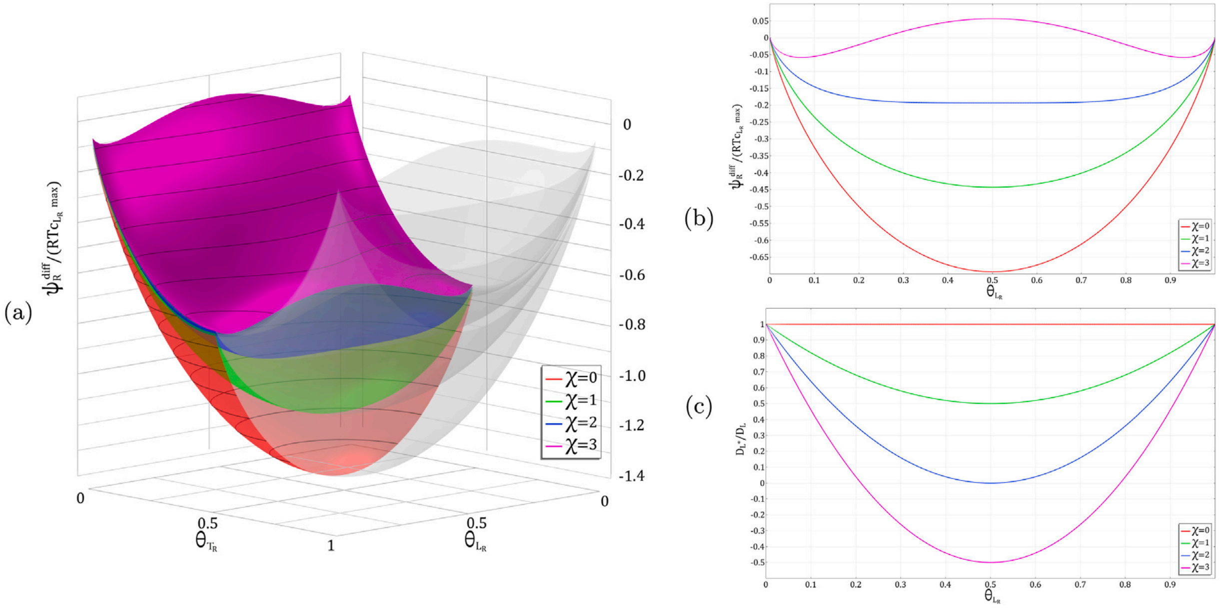

Fig. 9. (a) Three-dimensional representation of the normalized diffusive contribution to the Helmholtz free energy density, $\psi_R^{diff}/(RT\,c_{L_R}^{max})$, vs. the normalized concentrations of mobile and trapped species, θ_L and θ_T, for in-plane evolution, for $\theta_T = 0$, of (b) $\psi_R^{diff}/(RT\,c_{L_R}^{max})$ vs. θ_L, and (c) normalized *effective* diffusivity, $\mathbb{D}^*_L/\mathbb{D}_L$, vs. θ_L, for $\chi = 0,\ 1,\ 2,\ 3$. For $\chi > 2$, the chemical free energy is a double-well non-convex potential, and the normalized *effective* diffusivity can assume negative values.

phase segregation of mobile species occurs. Having set the saturation limit $c_{L_R}^{max} = 10^4\ \mathrm{mol/m^3}$, we observe that phase segregation may develop for $2000\ \mathrm{mol/m^3} \leq c_{L_R} \leq 8000\ \mathrm{mol/m^3}$, approximately, whereas the highest value of the concentration of mobile species reached in the simulations is $c_{L_R} \approx 650\ \mathrm{mol/m^3}$.

Density plots of concentrations c_{L_R} and c_{T_R} are shown at $t = 3600$ s in Fig. 10a–d, and e–h, respectively. Uninterrupted and irreversible trapping leads to the chemo-mechanical deformation of the particle, according to Eq. (132). The drop-like shape of the particle highlights the swelling after trapping, which becomes more pronounced at increasing values of χ. Higher values of the Flory–Huggins parameter induce higher concentrations of c_{T_R}, which localize in the apical point of the sphere as a result of the fast kinetics of chemical reaction (11), yielding the large reshaping of the particle.

Fig. 11a shows that the mass of species L increases as long as $\vec{h}_{L_R}$ enters the particle, reaching a peak at $t = 2700$ s. The higher χ the lower the mass implanted, manifesting the effect of χ on the trapping. The mass of trapped species increases in time, even after the external influx quits, in view of the continuous conversion of species L into T. As justified above, the mass of trapped species increases with the Flory–Huggins parameter χ.

10. Concluding remarks

A general framework that couples mass transport, chemical reactions with trapping, and finite strain thermo-mechanics has been presented. The formulation describes interstitial motion of free diffusive species in a hosting material; once trapped, species stay immobile, ceasing to contribute to mass transport and potentially inducing the swelling of the material. Elasto-plastic effects, as well as thermal evolution, are accounted for.

Kinematics is designed by means of a suitable multiplicative split of the deformation gradient. Mass balance equations are augmented with the rate of the chemical reaction, which portrays the conversion of mobile guest species to trapped species, and vice-versa, and a source term to describe injection or removal of mass. The enthalpy and the entropy contributions due to mass flux for the two laws of thermodynamics lead to the definition of the chemical potential as the sum of enthalpic and entropic contributions. In accordance with the multiplicative decomposition of the deformation gradient, the mechanical contribution to the entropy imbalance is additively split into chemo-thermo-elastic and inelastic parts, conveniently defined as a function of the chemo-thermo-elastic second Piola–Kirchhoff and Mandel stress tensors, respectively. The standard method of Coleman and Noll, and the assumption of Curie's symmetry principles, determine all thermodynamic prescriptions. The referential Helmholtz free energy density is chosen as a thermodynamic potential, and constitutively subjected to an additive decomposition to account for all processes involved in the material behavior. Such splitting drives the constitutive specifications of chemical potentials, heat and mass fluxes, and chemical kinetics. Governing equations, with associated Neumann and Dirichlet boundary conditions, are derived to complete the full coupling of the finite strain chemo-thermo-mechanics with trapping.

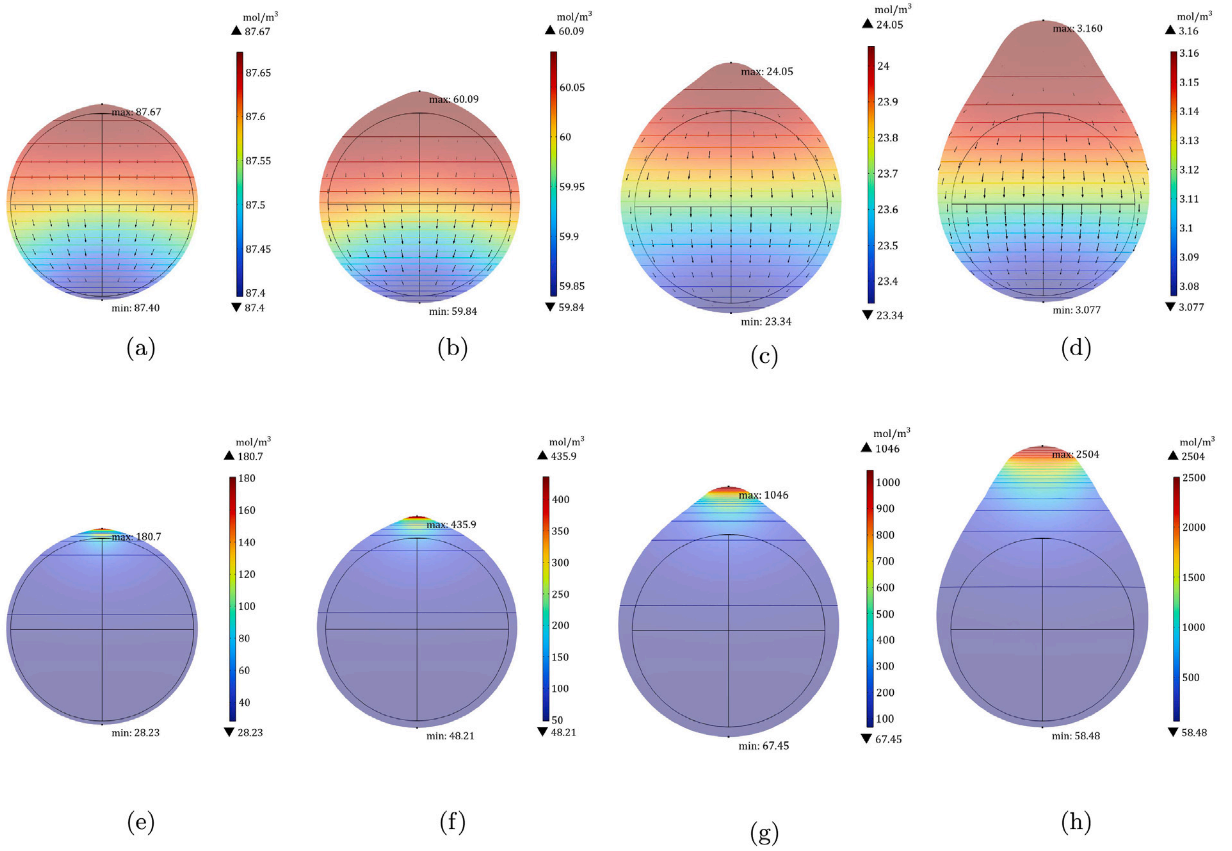

Fig. 10. Density plots of the concentration (a–d) c_{L_R} and (e–h) c_{T_R}, at $t = 3600$ s, for increasing values of the Flory–Huggins parameter, $\chi = 0,\ 1,\ 2,\ 3$, from left to right.

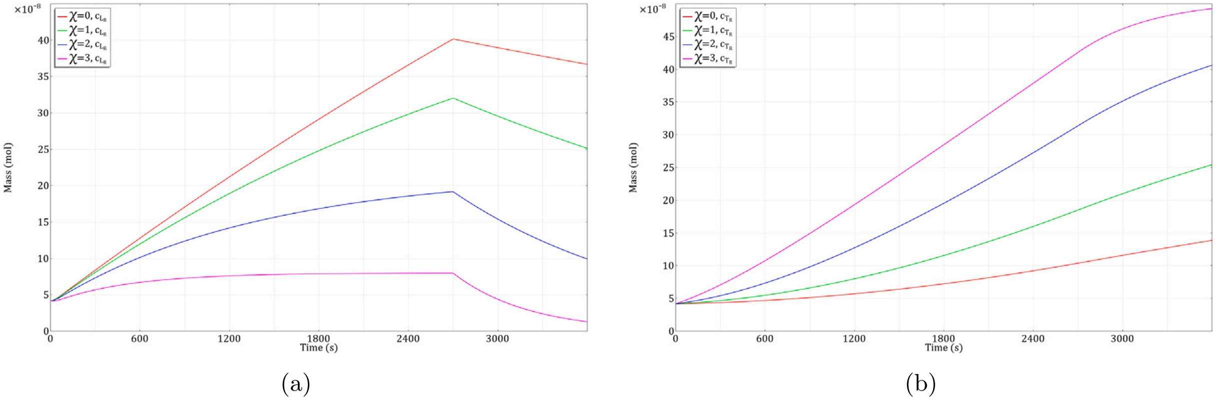

Fig. 11. (a) Mass of mobile species L and (b) of trapped species T as a function of time, for different values of the Flory–Huggins parameter: $\chi = 0,\ 1,\ 2,\ 3$.

A numerical study illustrated the chemo-transport-mechanical response of a particle subjected to a localized focused ion beam mass implantation (lithiation was considered in Takeuchi et al. (2016)), highlighting the reciprocal interactions among multi-physical processes. The reported volume change (factor of ≃ 2.3) points out how a multi-physical model limited to the realm of small deformations, as in Salvadori et al. (2018b), may not be representative of experimental reality. The trapping process cause large mechanical deformations, depending upon the concentration of species, the chemical kinetics, and the Flory–Huggins interaction parameter. A parametric study on the influence of χ on the chemo-mechanical response of the particle has been carried out.

Forthcoming publications will be devoted to further, and more specialized, high performance computational implementations of the proposed multi-physics framework, extending previously published works (Arricca et al., 2022; Serpelloni et al., 2022; Cabras et al., 2022a,b; Magri et al., 2022).

Declaration of competing interest

The authors declare that they have no known competing financial interests or personal relationships that could have appeared to influence the work reported in this paper.

Data availability

No data was used for the research described in the article.

Acknowledgments

This paper has been funded by the Mechanobiology research center at UNIBS, Italy, for which authors express their gratitude to the companies Copan, Antares Vision, Comipont, and the Ferriera Valsabbia foundation. The authors acknowledge the use of COMSOL at the University of California, Santa Barbara.

Appendix

A.1. Proof of Eq. (64)

The independence of the vector $\mathrm{Grad}\left[\,\mu_L\,\right] + {}^{\eta}\mu_L\,\mathrm{Grad}\,[\,T\,]$ upon the temperature gradient ca be shown be re-writing the chemical potential gradient of species L in the form

$$\begin{aligned}\mathrm{Grad}\left[\,\mu_L\,\right] &= \mathrm{Grad}\left[\frac{\partial\psi_R}{\partial c_{L_R}}\right] = \frac{\partial}{\partial c_{L_R}}\,\mathrm{Grad}\left[\psi_R\left(T, c_{L_R}, c_{T_R}, \mathbf{C}^{cte}\xi\right)\right]\\ &= \frac{\partial}{\partial c_{L_R}}\left(\frac{\partial\psi_R}{\partial T}\,\mathrm{Grad}\,[\,T\,] + \frac{\partial\psi_R}{\partial c_{L_R}}\,\mathrm{Grad}\left[\,c_{L_R}\,\right] + \frac{\partial\psi_R}{\partial c_{T_R}}\,\mathrm{Grad}\left[\,c_{T_R}\,\right] + \frac{\partial\psi_R}{\partial\mathbf{C}^{cte}} : \mathrm{Grad}\left[\,\mathbf{C}^{cte}\,\right]\right.\\ &\left.+\frac{\partial\psi_R}{\partial\xi} : \mathrm{Grad}\,[\,\xi\,]\right)\\ &= \frac{\partial^2\psi_R}{\partial c_{L_R}\partial T}\,\mathrm{Grad}\,[\,T\,] + \frac{\partial^2\psi_R}{\partial c_{L_R}^2}\,\mathrm{Grad}\left[\,c_{L_R}\,\right] + \frac{\partial^2\psi_R}{\partial c_{L_R}\partial c_{T_R}}\,\mathrm{Grad}\left[\,c_{T_R}\,\right]\\ &+ \frac{\partial^2\psi_R}{\partial c_{L_R}\partial\mathbf{C}^{cte}} : \mathrm{Grad}\left[\,\mathbf{C}^{cte}\,\right] + \frac{\partial^2\psi_R}{\partial c_{L_R}\partial\xi} : \mathrm{Grad}\,[\,\xi\,]\ ,\end{aligned} \tag{140}$$

and the term ${}^{\eta}\mu_L\,\mathrm{Grad}\,[\,T\,]$, according to the definition shown in Eq. (62a), as

$${}^{\eta}\mu_L\,\mathrm{Grad}\,[\,T\,] = -\frac{\partial^2\psi_R}{\partial c_{\alpha_R}\partial T}\,\mathrm{Grad}\,[\,T\,]\,. \tag{141}$$

Combination of Eqs. (140) and (141) yields

$$\begin{aligned}\mathrm{Grad}\left[\,\mu_L\,\right] + {}^{\eta}\mu_L\,\mathrm{Grad}\,[\,T\,] = &\frac{\partial^2\psi_R}{\partial c_{L_R}^2}\,\mathrm{Grad}\left[\,c_{L_R}\,\right] + \frac{\partial^2\psi_R}{\partial c_{L_R}\partial c_{T_R}}\,\mathrm{Grad}\left[\,c_{T_R}\,\right] + \frac{\partial^2\psi_R}{\partial c_{L_R}\partial\mathbf{C}^{cte}} : \mathrm{Grad}\left[\,\mathbf{C}^{cte}\,\right]\\ &+ \frac{\partial^2\psi_R}{\partial c_{L_R}\partial\xi} : \mathrm{Grad}\,[\,\xi\,]\,.\end{aligned} \tag{142}$$

A.2. The generalized heat equation

To derive the generalized heat equation, recall the referential localized energy balance (29), and the split of the mechanical contribution $\mathbf{P} : \dot{\mathbf{F}}$ into chemo-thermo-elastic and inelastic terms given by Eq. (52). It holds that

$$\begin{aligned}\frac{\mathrm{d}u_R}{\mathrm{d}t} = &\frac{1}{2}\,J^p\,\mathbf{S}^{cte} : \dot{\mathbf{C}}^{cte} + J^p\,\mathbf{M}^{cte} : \boldsymbol{l}^p + s_{q_R} - \mathrm{Div}\left[\,\vec{q}_R\,\right] + {}^{u}\mu_L\,\frac{\partial c_{L_R}}{\partial t} - \vec{h}_{L_R}\cdot\mathrm{Grad}\left[\,{}^{u}\mu_L\,\right] + {}^{u}\mu_T\,\frac{\partial c_{T_R}}{\partial t}\\ &+ \left({}^{u}\mu_L - {}^{u}\mu_T\right)\,w_R^{(11)}.\end{aligned} \tag{143}$$

By means of the time derivative of ψ_R (53) and Eq. (56),

$$\begin{aligned}T\,\frac{\mathrm{d}\eta_R}{\mathrm{d}t} - \frac{\mathrm{d}u_R}{\mathrm{d}t} &= -\frac{\mathrm{d}\psi_R}{\mathrm{d}t} - \frac{\partial T}{\partial t}\,\eta_R\\ &= -\frac{\partial\psi_R}{\partial\mathbf{C}^{cte}} : \frac{\partial\mathbf{C}^{cte}}{\partial t} - \frac{\partial\psi_R}{\partial c_{L_R}}\,\frac{\partial c_{L_R}}{\partial t} - \frac{\partial\psi_R}{\partial c_{T_R}}\,\frac{\partial c_{T_R}}{\partial t} - \frac{\partial\psi_R}{\partial T}\,\frac{\partial T}{\partial t} - \frac{\partial\psi_R}{\partial\xi} : \frac{\partial\xi}{\partial t} - \frac{\partial T}{\partial t}\,\eta_R.\end{aligned} \tag{144}$$

Taking advantage of the definition of the inelastic stress (57) and from the thermodynamic prescriptions for $\mathbf{S}^{cte}$, η_R, μ_L and μ_T, given by Eqs. (59), we substitute the partial derivatives of ψ_R in Eq. (144),

$$\begin{aligned} T\,\frac{\mathrm{d}\eta_R}{\mathrm{d}t} - \frac{\mathrm{d}u_R}{\mathrm{d}t} &= -\frac{\mathrm{d}\psi_R}{\mathrm{d}t} - \frac{\partial T}{\partial t}\,\eta_R \\ &= -\frac{1}{2}\,J^p\,\mathbf{S}^{cte} : \frac{\partial \mathbf{C}^{cte}}{\partial t} - \mu_L\,\frac{\partial c_{L_R}}{\partial t} - \mu_T\,\frac{\partial c_{T_R}}{\partial t} + \eta_R\,\frac{\partial T}{\partial t} + \chi : \frac{\partial \xi}{\partial t} - \frac{\partial T}{\partial t}\,\eta_R \\ &= -\frac{1}{2}\,J^p\,\mathbf{S}^{cte} : \frac{\partial \mathbf{C}^{cte}}{\partial t} - \mu_L\,\frac{\partial c_{L_R}}{\partial t} - \mu_T\,\frac{\partial c_{T_R}}{\partial t} + \chi : \frac{\partial \xi}{\partial t}\,, \end{aligned} \tag{145}$$

from which the following form of the referential energy balance arises

$$T\,\frac{\mathrm{d}\eta_R}{\mathrm{d}t} = -T\,\frac{\partial}{\partial T}\,\frac{\mathrm{d}\psi_R}{\mathrm{d}t} = \frac{\mathrm{d}u_R}{\mathrm{d}t} - \frac{1}{2}\,J^p\,\mathbf{S}^{cte} : \frac{\partial \mathbf{C}^{cte}}{\partial t} - \mu_L\,\frac{\partial c_{L_R}}{\partial t} - \mu_T\,\frac{\partial c_{T_R}}{\partial t} + \chi : \frac{\partial \xi}{\partial t}. \tag{146}$$

Taking advantage of Eq. (143),

$$\begin{aligned} T\,\frac{\mathrm{d}\eta_R}{\mathrm{d}t} &= -\,T\,\frac{\partial}{\partial T}\,\frac{\mathrm{d}\psi_R}{\mathrm{d}t} \\ &= \frac{1}{2}\,J^p\,\mathbf{S}^{cte} : \frac{\partial \mathbf{C}^{cte}}{\partial t} + J^p\,\mathbf{M}^{cte} : \boldsymbol{l}^p + s_{q\,R} - \operatorname{Div}\left[\vec{q}_R\right] + {}^{u}\mu_L\,\frac{\partial c_{L_R}}{\partial t} - \vec{h}_{L_R} \cdot \operatorname{Grad}\left[{}^{u}\mu_L\right] \\ &+ {}^{u}\mu_T\,\frac{\partial c_{T_R}}{\partial t} + \left({}^{u}\mu_L - {}^{u}\mu_T\right)\,w_R^{(11)} - \frac{1}{2}\,\mathbf{S}^{cte} : \dot{\mathbf{C}}^{cte} - \mu_L\,\frac{\partial c_{L_R}}{\partial t} - \mu_T\,\frac{\partial c_{T_R}}{\partial t} + \chi : \frac{\partial \xi}{\partial t}\,, \end{aligned} \tag{147}$$

hence

$$\begin{aligned} -T\,\frac{\partial}{\partial T}\,\frac{\mathrm{d}\psi_R}{\mathrm{d}t} &= J^p\,\mathbf{M}^{cte} : \boldsymbol{l}^p + s_{q\,R} - \operatorname{Div}\left[\vec{q}_R\right] + \left({}^{u}\mu_L - \mu_L\right)\,\frac{\partial c_{L_R}}{\partial t} - \vec{h}_{L_R} \cdot \operatorname{Grad}\left[{}^{u}\mu_L\right] \\ &+ \left({}^{u}\mu_T - \mu_T\right)\,\frac{\partial c_{T_R}}{\partial t} + \left({}^{u}\mu_L - {}^{u}\mu_T\right)\,w_R^{(11)} + \chi : \frac{\partial \xi}{\partial t}. \end{aligned} \tag{148}$$

The left-hand side term of Eq. (148) can be re-written by means of the time derivative of the Helmholtz free energy density, and in view of its functional dependence (56) results in

$$\begin{aligned} -T\,\frac{\partial}{\partial T}\,\frac{\mathrm{d}\psi_R}{\mathrm{d}t} &= -T\,\frac{\partial}{\partial T}\left(\frac{\partial \psi_R}{\partial \mathbf{C}^{cte}} : \frac{\partial \mathbf{C}^{cte}}{\partial t} + \frac{\partial \psi_R}{\partial c_{L_R}}\,\frac{\partial c_{L_R}}{\partial t} + \frac{\partial \psi_R}{\partial c_{T_R}}\,\frac{\partial c_{T_R}}{\partial t} + \frac{\partial \psi_R}{\partial T}\,\frac{\partial T}{\partial t} + \frac{\partial \psi_R}{\partial \xi} : \frac{\partial \xi}{\partial t}\right) \\ &= -T\left(\frac{\partial^2 \psi_R}{\partial T\,\partial \mathbf{C}^{cte}} : \frac{\partial \mathbf{C}^{cte}}{\partial t} + \frac{\partial^2 \psi_R}{\partial T\,\partial c_{L_R}}\,\frac{\partial c_{L_R}}{\partial t} + \frac{\partial^2 \psi_R}{\partial T\,\partial c_{T_R}}\,\frac{\partial c_{T_R}}{\partial t} + \frac{\partial^2 \psi_R}{\partial T^2}\,\frac{\partial T}{\partial t}\right. \\ &\left. + \frac{\partial^2 \psi_R}{\partial T\,\partial \xi} : \frac{\partial \xi}{\partial t}\right). \end{aligned} \tag{149}$$

Equating Eqs. (148) and (149) to re-write the terms

$$-T\,\frac{\partial^2 \psi_R}{\partial T^2}\,\frac{\partial T}{\partial t} + \operatorname{Div}\left[\vec{q}_R\right]$$

we find that

$$\begin{aligned} -T\,\frac{\partial^2 \psi_R}{\partial T^2}\,\frac{\partial T}{\partial t} + \operatorname{Div}\left[\vec{q}_R\right] &= J^p\,\mathbf{M}^{cte} : \boldsymbol{l}^p + s_{q\,R} + \left({}^{u}\mu_L - \mu_L\right)\,\frac{\partial c_{L_R}}{\partial t} - \vec{h}_{L_R} \cdot \operatorname{Grad}\left[{}^{u}\mu_L\right] \\ &+ \left({}^{u}\mu_T - \mu_T\right)\,\frac{\partial c_{T_R}}{\partial t} + \left({}^{u}\mu_L - {}^{u}\mu_T\right)\,w_R^{(11)} + \chi : \frac{\partial \xi}{\partial t} \\ &+ T\,\frac{\partial^2 \psi_R}{\partial T\,\partial \mathbf{C}^{cte}} : \frac{\partial \mathbf{C}^{cte}}{\partial t} + T\,\frac{\partial^2 \psi_R}{\partial T\,\partial c_{L_R}}\,\frac{\partial c_{L_R}}{\partial t} + T\,\frac{\partial^2 \psi_R}{\partial T\,\partial c_{T_R}}\,\frac{\partial c_{T_R}}{\partial t} \\ &+ T\,\frac{\partial^2 \psi_R}{\partial T\,\partial \xi} : \frac{\partial \xi}{\partial t} \\ &= J^p\,\mathbf{M}^{cte} : \boldsymbol{l}^p + s_{q\,R} + \left({}^{u}\mu_L - \mu_L + T\,\frac{\partial^2 \psi_R}{\partial T\,\partial c_{L_R}}\right)\frac{\partial c_{L_R}}{\partial t} \\ &- \vec{h}_{L_R} \cdot \operatorname{Grad}\left[{}^{u}\mu_L\right] + \left({}^{u}\mu_T - \mu_T + T\,\frac{\partial^2 \psi_R}{\partial T\,\partial c_{T_R}}\right)\frac{\partial c_{T_R}}{\partial t} \\ &+ \left({}^{u}\mu_L - {}^{u}\mu_T\right)\,w_R^{(11)} + \left(\chi + T\,\frac{\partial^2 \psi_R}{\partial T\,\partial \xi}\right) : \frac{\partial \xi}{\partial t} + T\,\frac{\partial^2 \psi_R}{\partial T\,\partial \mathbf{C}^{cte}} : \frac{\partial \mathbf{C}^{cte}}{\partial t}\,, \end{aligned} \tag{150}$$

In respect of the definition of μ_α given by Eq. (39), and according to the specification for ${}^{\eta}\mu_\alpha$ defined in Eq. (62a), the two parenthetical terms that multiply the time derivatives of the referential concentration of species in Eq. (150) are null, hence

$$T\,\frac{\partial^2\,\psi_R}{\partial c_{\alpha_R}\,\partial T} + {}^{u}\mu_\alpha - \mu_\alpha = 0. \tag{151}$$

Therefore

$$
\begin{aligned}
-T\,\frac{\partial^2\psi_R}{\partial T^2}\,\frac{\partial T}{\partial t}+\mathrm{Div}\left[\,\vec{q}_R\,\right]=T\,\frac{\partial^2\psi_R}{\partial T\partial\mathbf{C}^{cte}}\,:\,\frac{\partial\mathbf{C}^{cte}}{\partial t}+J^p\,\mathbf{M}^{cte}\,:\,\boldsymbol{l}^p+s_{q\,R}-\vec{h}_{L_R}\cdot\mathrm{Grad}\left[\,{}^u\mu_L\,\right]\\
+\left(\chi+T\,\frac{\partial^2\psi_R}{\partial T\partial\xi}\right)\,:\,\frac{\partial\xi}{\partial t}+\left({}^u\mu_L-{}^u\mu_T\right)w_R^{(11)}.
\end{aligned}
\tag{152}
$$

Lastly, by means of the constitutive prescriptions for the Fick's and Fourier's laws shown in Eqs. (116a) and (116b), respectively, the following generalized heat equation arises

$$
\begin{aligned}
-T\,\frac{\partial^2\psi_R}{\partial T^2}\,\frac{\partial T}{\partial t}-\mathrm{Div}\left[\,\mathbb{K}\ \ \mathrm{grad}\,[\,T\,]\,\right]=T\,\frac{\partial^2\psi_R}{\partial T\partial\mathbf{C}^{cte}}\,:\,\frac{\partial\mathbf{C}^{cte}}{\partial t}+J^p\,\mathbf{M}^{cte}\,:\,\boldsymbol{l}^p+s_{q\,R}\\
+\left(\chi+T\,\frac{\partial^2\psi_R}{\partial T\partial\xi}\right)\,:\,\frac{\partial\xi}{\partial t}\\
+\mathbf{M}_{L_R}(c_{L_R})\,\left(\mathrm{Grad}\left[\,\mu_L\,\right]+{}^\eta\mu_L\,\mathrm{Grad}\,[\,T\,]\right)\cdot\mathrm{Grad}\left[\,{}^u\mu_L\,\right]\\
+\left({}^u\mu_L-{}^u\mu_T\right)w_R^{(11)}
\end{aligned}
\tag{153}
$$

with ${}^u\mu_L$ and ${}^u\mu_T$ defined by Eq. (62b).

References

Anand, L., 2012. A cahn-hilliard-type theory for species diffusion coupled with large elastic-plastic deformations. J. Mech. Phys. Solids 60 (12), 1983–2002.

Arricca, M., Salvadori, A., Bonanno, C., Serpelloni, M., 2022. Modeling receptor motility along advecting lipid membranes. Membranes 12 (7), 652.

Bacca, M., McMeeking, R.M., 2017. A viscoelastic constitutive law for hydrogels. Meccanica 52, 3345–3355.

Bacca, M., Saleh, O.A., McMeeking, R.M., 2019. Contraction of polymer gels created by the activity of molecular motors. Soft Matter 15, 4467–4475.

Bell, G.I., 1978. Models for the specific adhesion of cells to cells. Science 200 (4342), 618–627.

Bohn, E., Eckl, T., Kamlah, M., McMeeking, R.M., 2013. A model for lithium diffusion and stress generation in an intercalation storage particle with phase change. J. Electrochem. Soc. 160 (10), A1638–A1652. http://dx.doi.org/10.1149/2.011310jes.

Boulbitch, A., Guttenberg, Z., Sackmann, E., 2001. Kinetics of membrane adhesion mediated by ligand-receptor interaction studied with a biomimetic system. Biophys. J. 81 (5), 2743–2751.

Cabras, L., Danilov, D., Subber, W., Oancea, V., Salvadori, A., 2022a. A two-mechanism and multiscale compatible approach for solid state electrolytes of (li-ion) batteries. J. Energy Storage 48, 103842.

Cabras, L., Serpelloni, M., Salvadori, A., 2022b. Electro-chemo-mechanics of solid state batteries with lithium plating and stripping. Front. Mater. 1052617.

Cheng, Q.H., Liu, P., Gao, H.J., Zhang, Y.W., 2009. A computational modeling for micropipette-manipulated cell detachment from a substrate mediated by receptor-ligand binding. J. Mech. Phys. Solids 57, 205–220.

Damioli, V., Salvadori, A., Beretta, G.P., Ravelli, C., Mitola, S., 2017. Multi-physics interactions drive VEGFR2 relocation on endothelial cells. Sci. Rep. UK 7 (1), 16700.

De Groot, S.R., Mazur, P., 1984. Non-Equilibrium Thermodynamics. Dover.

DeHoff, R., 2006. Thermodynamic in Material Science. CRC Press - Taylor and Francis.

Deshpande, V.S., McMeeking, R.M., Evans, A.G., 2007. A model for the contractility of the cytoskeleton including the effects of stress-fiber formation and dissociation. Proc. R. Soc. Lond. Ser. A 463, 787–815.

Deshpande, V.S., Mrksich, M., McMeeking, R.M., Evans, A.G., 2008. A bio-mechanical model for coupling cell contractility with focal adhesion formation. J. Mech. Phys. Solids 56, 1484–1510.

Di Leo, C., Rejovitzky, E., Anand, L., 2014. A cahn-hilliard-type phase-field theory for species diffusion coupled with large elastic deformations: Application to phase-separating li-ion electrode materials. J. Mech. Phys. Solids 70, 1–29.

Doll, S., Schweizerhof, K., 2000. On the development of volumetric strain energy functions. ASME J. Appl. Mech. 67, 17–21.

Drozdov, A.D., 2014. Viscoplastic response of electrode particles in li-ion batteries driven by insertion of lithium. Int. J. Solids Struct. 51, 690–705.

Freund, L.B., Lin, Y., 2004. The role of binder mobility in spontaneous adhesive contact and implication for cell adhesion. J. Mech. Phys. Solids 52, 2455–2472.

Ganser, M., Hildenbrand, F.E., Kamlah, M., McMeeking, R.M., 2019. A finite strain electro-chemo-mechanical theory for ion transport with application to binary solid electrolytes. J. Mech. Phys. Solids 125, 681–713.

Golestaneh, A.F., Nadler, B., 2016. Modeling of cell adhesion and deformation mediated by receptor-ligand interactions. Biomech. Model Mechanobiol. 15, 371–387.

Gurtin, M.E., Fried, E., Anand, L., 2010. The Mechanics and Thermodynamics of Continua. Cambridge University Press.

Hajikhani, A., Wriggers, P., Marino, M., 2021. Chemo-mechanical modelling of swelling and crosslinking reaction kinetics in alginate hydrogels: A novel theory and its numerical implementation. J. Mech. Phys. Solids 153.

Hirth, J.P., 1980. Effects of hydrogen on the properties of iron and steel. Metall. Trans. A 11A, 861–876.

Holzapfel, G., 2001. Nonlinear Solid Mechanics: A Continuum Approach for Engineering. John Wiley & Sons, Ltd..

Krom, A.H.M., Bakker, A., 2000. Hydrogen trapping models in steel. Metall. Mater. Trans. B 31B, 1475–1482.

Krom, A.H.M., Koers, R.W.J, Bakker, A., 1999. Hydrogen transport near a blunting crack tip. J. Mech. Phys. Solids 47, 971–992.

Kumnick, A.J., Johnson, H.H, 1980. Deep trapping states for hydrogen in deformed iron. Acta Metall. Mater. 28, 33–39.

Larche, F., Cahn, J.W., 1973. A linear theory of thermochemical equilibrium under stress. Acta Metall. Mater. 21, 1051–1063.

Larche, F., Cahn, J.W., 1978. Non linear theory of thermochemical equilibrium under stress. Acta Metall. Mater. 26, 53–60.

Liu, X.H., Wang, J.W., Huang, S., Fan, F., Huang, X., Liu, Y., Krylyuk, S., Yoo, J., Dayeh, S.A., Davydov, A.V., Mao, S.X., Picraux, S.T., Zhang, S., Li, J., Zhu, T., Huang, J.Y., 2012. In situ atomic-scale imaging of electrochemical lithiation in silicon. Nat. Nanotechnol. 7, 749–756.

Liu, P., Zhang, Y.W., Cheng, Q.H., Lu, C., 2007. Simulation of the spreading of a vesicle on a substrate surface mediated by receptor-ligand binding. J. Mech. Phys. Solids 55 (6), 1166–1181.

Lucantonio, A., Teresi, L., DeSimone, A., 2016. Continuum theory of swelling material surfaces with applications to thermo-responsive gel membranes and surface mass transport. J. Mech. Phys. Solids 89, 96–109.

Magri, M., Boz, B., Cabras, L., Salvadori, A., 2022. Quantitative investigation of the influence of electrode morphology in the electro-chemo-mechanical response of li-ion batteries. Electrochim. Acta 405, 139778.

McDowell, M.T., Lee, S.W., Harris, J.T., Korgel, B.A., Wang, C., Nix, W.D., Cui, Y., 2013. In situ TEM of two-phase lithiation of amorphous silicon nanospheres. Nano Lett. 13 (2), 758–764.

McMeeking, R.M., Deshpande, V.S., 2017. A bio-chemo-mechanical model for cell contractility, adhesion, signaling, and stress-fiber remodeling. In: Holzapfel, G.A., Ogden, R.W. (Eds.), Biomechanics: Trends in Modeling and Simulation. In: Studies in Mechanobiology, Tissue Engineering and Biomaterials, vol. 20, Springer, pp. 53–81.

McNabb, A., Foster, P.K., 1963. A new analysis of the diffusion of hydrogen in iron and ferritic steels. Trans. Metall. Soc. AIME 227, 618–627.

Narayan, S., Anand, L., 2022. A coupled electro-chemo-mechanical theory for polyelectrolyte gels with application to modeling their chemical stimuli-driven swelling response. J. Mech. Phys. Solids 159.

Oriani, R.A., 1970. The diffusion and trapping of hydrogen in steel. Acta Metall. Mater. 18 (1), 147–157.

Paolucci, S., 2016. Continuum Mechanics and Thermodynamics of Matter. Cambridge University Press.

Pharr, M., Zhao, K., Wang, X., Suo, Z., Vlassak, J.J., 2012. Kinetics of initial lithiation of crystalline silicon electrodes of lithium-ion batteries. Nano Lett. 12, 5039–5047.

Prigogine, I., 1977. Nobel lecture: Time, structure and fluctuations.

Rosakis, P., Rosakis, A.J., Ravichandran, G., Hodowany, J., 2000. A thermodynamic internal variable model for the partition of plastic work into heat and stored energy in metals. J. Mech. Phys. Solids 48, 581–607.

Salvadori, A., Damioli, V., Ravelli, C., Mitola, S., 2018a. Modeling and simulation of VEGF receptors recruitment in angiogenesis. Math. Probl. Eng..

Salvadori, A., McMeeking, R.M., Grazioli, D., Magri, M., 2018b. A coupled model of transport-reaction-mechanics with trapping. Part I - small strain analysis. J. Mech. Phys. Solids 114, 1–30.

Serpelloni, Mattia, 2020. Response of Endothelial Cells to Angiogenic Stimuli: Experiments, Modeling and Simulations (Ph.D. thesis). University of Brescia.

Serpelloni, M., Arricca, M., Bonanno, C., Salvadori, A., 2021. Modeling cells spreading, motility, and receptors dynamics: a general framework. Acta Mech. Sin. 37 (6), 1013–1030.

Serpelloni, M., Arricca, M., Bonanno, C., Salvadori, A., 2022. Chemo-transport-mechanics in advecting membranes.. Int. J. Eng. Sci. 181 (1), 103746.

Serpelloni, M., Arricca, M., Damioli, V., Ravelli, C., Grillo, E., Mitola, S., Salvadori, A., 2020. A model of integrin and VEGF receptors recruitment on endothelial cells. In: Abali, B.E., Giorgio, I. (Eds.), Developments and Novel Approaches in Biomechanics and Metamaterials. Springer International Publishing, Cham, pp. 163–198.

Shell, S., 2015. Thermodynamics and Statistical Mechanics: An Integrated Approach. Cambridge University Press.

Shenoy, V.B., Freund, L.B., 2005. Growth and shape stability of a biological membrane adhesion complex in the diffusion-mediated regime. Proc. Natl. Acad. Sci. USA 102 (9), 3213–3218.

Simo, J.C., 1988a. A framework for finite strain elastoplasticity based on maximum plastic dissipation and the multiplicative decomposition: Part I. Continuum formulation. Comput. Methods Appl. Mech. Engrg. 66 (2), 199–219.

Simo, J.C., 1988b. A framework for finite strain elastoplasticity based on maximum plastic dissipation and the multiplicative decomposition. Part II: Computational aspects. Comput. Methods Appl. Mech. Engrg. 68 (1), 1–31.

Sofronis, P., McMeeking, R.M., 1989. Numerical analysis of hydrogen transport near a blunting crack tip. J. Mech. Phys. Solids 37 (317–350).

Steinmann, P., Scherer, M., Denzer, R., 2009. Secret and joy of configurational mechanics: From foundations in continuum mechanics to applications in computational mechanics. Z. Angew. Math. Mech. 89 (8).

Tadmor, E.B., Miller, R.E., Elliott, R.S., 2011. Continuum Mechanics and Thermodynamics: From Fundamental Concepts to Governing Equations. Cambridge University Press.

Takeuchi, S., McGehee, W.R., Schaefer, J.L., Wilson, T.M., Twedt, K.A., Chang, E.H., Soles, C.L., Oleshko, V.P., McClelland, J.J., 2016. Comparison of nanoscale focused ion beam and electrochemical lithiation in β-sn microspheres.. J. Electrochem. Soc. 163 (6), A1010–A1012.

Toribio, J., Kharin, V., 2015. A generalised model of hydrogen diffusion in metals with multiple trap types. Philos. mag. 95 (31), 3429–3451.

Vernerey, F.J., Farsad, M., 2014. A mathematical model of the coupled mechanisms of cell adhesion, contraction and spreading. J. Math. Biol. 68, 989–1022.

Wang, J.W., He, Y., Fan, F., Liu, X.H., Xia, S., Liu, Y., Harris, C.T., Li, H., Huang, J.Y., Mao, S.X., Zhu, T., 2013. Two-phase electrochemical lithiation in amorphous silicon. Nano Lett. 13 (2), 709–715.

Zhang, Q., White, R.E., 2007. Moving boundary model for the discharge of a $LiCoO_2$ electrode. J. Electrochem. Soc. 154 (6), A587–A596.

Zhao, K., Pharr, M., Wan, Q., Wang, W.L., Kaxiras, E., Vlassak, J.J., Suo, Z., 2012. Concurrent reaction and plasticity during initial lithiation of crystalline silicon in lithium-ion batteries. J. Electrochem. Soc. 159, A238–A243.

Zhong, Z., Qin, B., Chen, J., 2021. A coupled theory for soft materials at finite strain with heat conduction, diffusion and chemical reactions. Comput. Mater. Sci. 188.